Search for long-lived particles using displaced vertices and missing transverse momentum in proton-proton collisions at $\sqrt{s} = 13$ TeV

A. Hayrapetyan *et al.*[*]
(CMS Collaboration)

(Received 24 February 2024; accepted 9 April 2024; published 5 June 2024)

A search for the production of long-lived particles in proton-proton collisions at a center-of-mass energy of 13 TeV at the CERN LHC is presented. The search is based on data collected by the CMS experiment in 2016–2018, corresponding to a total integrated luminosity of 137 fb^{-1}. This search is designed to be sensitive to long-lived particles with mean proper decay lengths between 0.1 and 1000 mm, whose decay products produce a final state with at least one displaced vertex and missing transverse momentum. A machine learning algorithm, which improves the background rejection power by more than an order of magnitude, is applied to improve the sensitivity. The observation is consistent with the standard model background prediction, and the results are used to constrain split supersymmetry (SUSY) and gauge-mediated SUSY breaking models with different gluino mean proper decay lengths and masses. This search is the first CMS search that shows sensitivity to hadronically decaying long-lived particles from signals with mass differences between the gluino and neutralino below 100 GeV. It sets the most stringent limits to date for split-SUSY models and gauge-mediated SUSY breaking models with gluino proper decay length less than 6 mm.

DOI: 10.1103/PhysRevD.109.112005

I. INTRODUCTION

Many theoretical models beyond the standard model (SM) predict the existence of long-lived particles (LLPs) with measurable decay lengths. Examples include split supersymmetry (SUSY) [1–6], SUSY with weak R-parity violation [7–10], gauge-mediated SUSY breaking (GMSB) [11–13], stealth SUSY [14,15], hidden-valley models [16–18], and twin Higgs models [19–21]. New particles predicted by these models can be produced at the CERN LHC, and LLP searches provide an opportunity to discover particles that have not been excluded by previous searches.

The search presented here is sensitive to LLPs whose decays include multiple charged particles and one weakly interacting neutral particle. To target this signature, the search is designed to be sensitive to topologies that include missing transverse momentum ($p_{\mathrm{T}}^{\mathrm{miss}}$) and at least one displaced vertex. A displaced vertex is reconstructed by identifying charged-particle trajectories converging at a point in space that is at a measurable distance from the proton-proton (pp) interaction point. Reconstructed vertices are required to be within a transverse displacement of approximately 2 cm, which ensures they are composed of well-measured trajectories and eliminates the possibility of background vertices caused by SM particle interactions with the CMS beam pipe.

The ATLAS and CMS Collaborations have previously performed searches for LLPs in signatures with displaced vertices [22–26]. Those searches target LLPs that either decay at least 1 mm away from the interaction point or have most of their energy decay into SM particles. The search presented in this paper is designed to cover the gaps left by previous searches, which include a wider range of LLP mean proper decay lengths ($c\tau$), from 0.1 to 1000 mm, and LLPs in "compressed" scenarios, where most of the LLP energy is carried away by undetected weakly interacting particles.

This search includes several improvements over the previous CMS displaced vertex search [24]. One such improvement is the inclusion of events with as few as one displaced vertex. This allows sensitivity to new physics models with only one LLP in the final state. It also enhances sensitivity to beyond the SM scenarios in which the reconstruction of displaced vertices is challenging, such as models involving lower energy carried by charged particles in the final states or cases where only one of the LLP decays occurs within the detector. Although requiring only one displaced vertex increases the signal efficiency, it also includes more background events. To further discriminate signal and background events, the "interaction

[*]Full author list given at the end of the article.

Published by the American Physical Society under the terms of the Creative Commons Attribution 4.0 International license. Further distribution of this work must maintain attribution to the author(s) and the published article's title, journal citation, and DOI. Funded by SCOAP[3].

 © 2024 CERN, for the CMS Collaboration

network" (IN) [27,28], a machine learning (ML) algorithm, is introduced to improve the sensitivity to the target signature. An alternative selection without using ML was studied and found to have a factor of 8 more background events for smaller signal efficiency. In addition, this search includes events with an overall total transverse momentum (p_T) imbalance, making it sensitive to final states with a significantly smaller scalar sum of jet p_T. The search uses events collected in pp collisions at the LHC in 2016–2018, corresponding to an integrated luminosity of 137 fb^{-1}.

This analysis uses split SUSY and GMSB SUSY as benchmark signal models, as shown in Fig. 1. The split-SUSY model features pair-produced, long-lived gluinos ($\tilde{g}$) that each decay into two quarks (q) and a neutralino ($\tilde{\chi}$). In this model, the SUSY breaking scale (m_{SUSY}) is assumed to be $m_{\mathrm{SUSY}} \gg 10^6$ TeV [2], and all scalar masses are set to that scale, except for a single, fine-tuned, Higgs boson mass. The $\tilde{g}$ decays through a high-mass, virtual squark resulting in a long $\tilde{g}$ lifetime. In the GMSB SUSY model, $\tilde{g}$ are pair-produced and decay to a gluon and a nearly massless gravitino ($\tilde{G}$). The decay is suppressed by m_{SUSY}, and thus the $\tilde{g}$ is long-lived. The lifetime of the gluino in both models is given by

$$\tau \simeq 8\left(\frac{m_{\mathrm{SUSY}}}{10^6\ \mathrm{TeV}}\right)^4\left(\frac{1\ \mathrm{TeV}}{m_{\tilde{g}}}\right)^5\ \mathrm{s}, \tag{1}$$

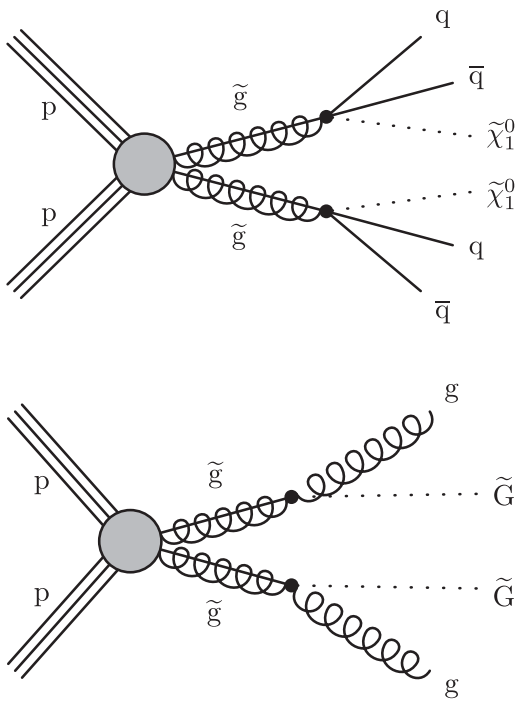

FIG. 1. Diagrams of the split-SUSY model (upper) and GMSB SUSY model (lower). In the split-SUSY model, a pair of long-lived gluinos is produced, and each decays to two quarks and one neutralino. In the GMSB SUSY model, a pair of long-lived gluinos is produced, and each decays to a gluon and a gravitino.

where $m_{\tilde{g}}$ corresponds to the $\tilde{g}$ mass [2,11]. Previously, the CMS Collaboration performed a search for the split-SUSY signal model [29]; however, the displaced signature was not targeted and the resulting large number of background events decreased the sensitivity.

The paper is organized as follows. Section II presents an overview of the CMS detector. Section III summarizes the data and simulation samples used in this search. We describe the displaced vertex reconstruction algorithm in Sec. IV, followed by the discussion of the ML algorithm in Sec. V. The event selection criteria and the determination of vertex reconstruction and ML tagging efficiency are summarized in Sec. VI. In Sec. VII, we explain the background estimation procedure based on control samples in data. Section VIII discusses systematic uncertainties in signal efficiency and background estimation. Section IX presents the results and statistical interpretation. Finally, the paper is summarized in Sec. X. Tabulated results are provided in the HEPData record for this analysis [30].

II. THE CMS DETECTOR

The central feature of the CMS apparatus is a superconducting solenoid of 6 m inner diameter, providing a magnetic field of 3.8 T. Within the solenoid volume are a silicon pixel and strip tracker, a lead tungstate crystal electromagnetic calorimeter (ECAL), and a brass and scintillator hadron calorimeter (HCAL), each composed of a barrel and two end cap sections. Forward calorimeters extend the pseudorapidity (η) coverage provided by the barrel and end cap detectors. A more detailed description of the CMS detector, together with a definition of the coordinate system used and the relevant kinematic variables, can be found in Ref. [31].

The silicon tracker used in 2016 measured charged particles within the range $|\eta| < 2.5$. For nonisolated particles within the ranges of $1 < p_T < 10$ GeV and $|\eta| < 1.4$, the track resolutions were typically 1.5% in p_T and 25–90 μm in the transverse impact parameter (d_{xy}) [32]. At the start of 2017, a new pixel detector was installed [33]; the upgraded tracker measured particles up to $|\eta| < 3.0$ with typical resolutions of 1.5% in p_T and 20–75 μm in d_{xy} [34] for nonisolated particles of $1 < p_T < 10$ GeV.

A particle-flow (PF) algorithm [35] aims to reconstruct and identify each individual particle in an event, with an optimized combination of information from the various elements of the CMS detector. The energy of photons is obtained from the ECAL measurement. The energy of electrons is determined from a combination of the electron momentum at the primary interaction vertex as determined by the tracker, the energy of the corresponding ECAL cluster, and the energy sum of all bremsstrahlung photons spatially compatible with originating from the electron track. The energy of muons is obtained from the curvature of the corresponding track. The energy of charged hadrons is determined from a combination of their momentum

measured in the tracker and the matching ECAL and HCAL energy deposits, corrected for the response function of the calorimeters to hadronic showers. Finally, the energy of neutral hadrons is obtained from the corresponding corrected ECAL and HCAL energies.

The primary vertex is taken to be the vertex corresponding to the hardest scattering in the event, evaluated using tracking information alone, as described in Sec. 9.4.1 of Ref. [36].

For each event, hadronic jets are clustered from PF candidates using the infrared- and collinear-safe anti-k_T algorithm [37,38] with a distance parameter of 0.4. Jet momentum is determined as the vectorial sum of all particle momenta in the jet and is found from simulation to be, on average, within 5% to 10% of the true momentum over the entire p_T spectrum and detector acceptance. Additional pp interactions within the same or nearby bunch crossings (referred to as pileup) can contribute additional tracks and calorimetric energy depositions to the jet momentum. To mitigate this effect, charged particles identified to be originating from pileup vertices are discarded and an offset correction is applied to correct for remaining contributions. Jet energy corrections are derived from simulation to bring the measured response of jets to that of particle level jets on average. *In situ* measurements of the momentum balance in dijet, photon + jet, Z + jet, and multijet events are used to account for any residual differences in the jet energy scale between data and simulation [39]. The jet energy resolution amounts typically to 15%–20% at 30 GeV, 10% at 100 GeV, and 5% at 1 TeV [39]. Additional selection criteria are applied to each jet to remove jets potentially dominated by anomalous contributions from various subdetector components or reconstruction failures [40].

The $\vec{p}_T^{\,\text{miss}}$ is computed as the negative vector p_T sum of all the PF candidates except muons in an event, and its magnitude is denoted as p_T^{miss} [41]. The $\vec{p}_T^{\,\text{miss}}$ is modified to account for corrections to the energy scale of the reconstructed jets in the event. Anomalous events with high p_T^{miss} can be due to a variety of reconstruction failures, detector malfunctions, or noncollision backgrounds. Such events are rejected by event filters that are designed to identify more than 85%–90% of the spurious high-p_T^{miss} events with a mistagging rate less than 0.1% [41].

Events of interest are selected using a two-tiered trigger system. The first level, referred to as the level-1 (L1) trigger, is composed of custom hardware processors and uses information from the calorimeters and muon detectors to select events at a rate of around 100 kHz within a fixed latency of about 4 μs [42]. The second level, known as the high-level trigger, consists of a farm of processors running a version of the full event reconstruction software optimized for fast processing, and reduces the event rate to around 1 kHz before data storage [43].

III. EVENT SAMPLES AND PRESELECTION

Events in both data and simulation are selected using a trigger requiring $p_T^{\text{miss}} > 120$ GeV. Events are further required to pass a set of quality filters [41] to reduce the possibility of mismeasuring p_T^{miss} and to have a well-reconstructed primary vertex. In addition, an offline requirement of $p_T^{\text{miss}} > 200$ GeV is applied to ensure consistent trigger efficiencies in data and simulation. These selections are referred to as event preselection criteria. Since the CMS detector operated under different conditions during successive data-taking periods, events collected in 2016, 2017, and 2018 are analyzed separately.

Signal events are simulated using PYTHIA 8.240 [44] with the CP2 tune [45] and the NNPDF3.1 leading-order (LO) [46] set of parton distribution functions (PDFs). The gluino production cross sections are then normalized to next-to-next-to-LO (NNLO) in quantum chromodynamics (QCD) and next-to-next-to-leading-logarithm (NNLL) soft-gluon resummation precision [47]. In order to account for possible kinematic effects of bound state formation, production of bound states that include a gluino is modeled with PYTHIA. The probability of forming a bound state of gluinos alone is set to the default value of 0.1. Since the search targets only displaced vertices within the beam pipe, material interactions with LLPs and their potential bound states are not considered. The split-SUSY samples are generated for various $m_{\tilde{g}}$ hypotheses in the range from 1200 to 2600 GeV, with the mass splitting between the $\tilde{g}$ and $\tilde{\chi}$ ranging from 20 to 800 GeV and the gluino $c\tau$ ranging from 0.1 to 1000 mm. The GMSB SUSY samples are generated with $m_{\tilde{g}}$ ranging from 1800 to 2800 GeV and the gluino $c\tau$ ranging from 0.1 to 1000 mm.

The dominant background processes include jets produced through the strong interaction, referred to as QCD events, and $t\bar{t}$. Other contributions arise from W and Z boson production in association with jets (W/Z + jets), single top quark production, and diboson production (WW, WZ, and ZZ). The QCD and W/Z + jets events are generated using MADGRAPH 5_aMC@NLO 2.6.5 [48] at LO in QCD, with the MLM [49] prescription of matching jets from matrix element calculations to those from parton showers. The $t\bar{t}$ events are generated using MADGRAPH 5_aMC@NLO 2.6.1 [48] at next-to-LO (NLO), with the FxFx [50] prescription of jet matching. Single top quark production is generated using POWHEG [51–55] (version 2.0 for t-channel and 1.0 for tW-channel production) at NLO in QCD and the diboson processes are generated using PYTHIA 8.240. The NNPDF3.1 NNLO [56] PDF set is used for all background processes. The background event generators are interfaced with PYTHIA to model the parton showering and fragmentation. The PYTHIA parameters affecting the description of the underlying event are set to the CP5 tune [45].

All generated events are processed through a simulation of the CMS detector based on GEANT [57] and are

reconstructed with the same algorithms as used for data. Simulated minimum bias events are superimposed on the hard interaction to describe the effect of pileup, and samples are weighted to match the pileup distribution observed in data.

IV. VERTEX RECONSTRUCTION

A detailed description of the displaced vertex reconstruction algorithm can be found in Ref. [24]. The displaced vertices are constructed from tracks. A set of quality criteria is applied to remove tracks with large reconstruction uncertainty, and a displacement criterion is applied to reduce the contribution of tracks from prompt SM processes. The quality requirements include $p_{\mathrm{T}} > 1$ GeV, at least one associated detector hit measured by the innermost layer of the pixel detector, at least two associated detector hits measured by the pixel detector, and at least six associated detector hits measured by the silicon strip detector. The displacement criterion used is based on d_{xy} measured with respect to the beam axis and its uncertainty ($\sigma_{d_{\mathrm{xy}}}$). In this search, the tracks selected to construct vertices are required to have $|d_{\mathrm{xy}}/\sigma_{d_{\mathrm{xy}}}| > 4$.

Each pair of selected tracks is used to construct a vertex using the Kalman filtering approach [58–60], and the vertex is considered valid if its χ^2 per degree of freedom is less than five. These reconstructed vertices then undergo an iterative merging procedure. This procedure utilizes the significance, defined as the ratio of a quantity and its uncertainty, of the 3D distance between vertices (d_{vv} and $\sigma_{d_{\mathrm{vv}}}$), $|d_{\mathrm{vv}}/\sigma_{d_{\mathrm{vv}}}|$, and the significance of the 3D impact parameter between tracks and vertices (d_{tv} and $\sigma_{d_{\mathrm{tv}}}$), $|d_{\mathrm{tv}}/\sigma_{d_{\mathrm{tv}}}|$. First, for each pair of vertices that share at least one track and have $|d_{\mathrm{vv}}/\sigma_{d_{\mathrm{vv}}}| < 4$, a new vertex is fit by the Kalman filtering method using all tracks associated with the pair of vertices. If the resulting vertex satisfies the χ^2 requirement, the pair of vertices is replaced by a single merged vertex. If not, the vertices are not merged and the shared track is assigned to one or neither of the two vertices according to the following arbitration criteria. If $|d_{\mathrm{tv}}/\sigma_{d_{\mathrm{tv}}}|$ formed from either of the vertices is greater than five, the track is dropped from that vertex; if $|d_{\mathrm{tv}}/\sigma_{d_{\mathrm{tv}}}|$ formed from both vertices is less than 1.5, the track is assigned to the vertex with the most tracks; otherwise, the track is assigned to the vertex that has the smaller $|d_{\mathrm{tv}}/\sigma_{d_{\mathrm{tv}}}|$. The resulting vertices then replace the original vertices if they meet the χ^2 requirement. This process is repeated until no vertices share tracks.

The final step of the vertex reconstruction aims to suppress ones in which tracks from different primary vertices coincidentally overlap. For each displaced vertex, we repeat the vertex fit with one track removed at a time and calculate the resulting change along the beam axis. If the vertex position along the beam axis shifts by more than 50 μm, which was chosen to maximize signal significance in Ref. [24], the track is removed from the vertex, and the procedure is iteratively repeated with the remaining tracks. The procedure stops if there are only two tracks in the vertex. All resulting vertices are required to satisfy the χ^2 requirement.

A set of selection criteria, which is similar to that of Ref. [24], is applied to the vertices in order to suppress vertices that arise from SM processes. First, the number of tracks in each vertex, n_{track}, must be ≥ 3. To suppress vertices from material interactions, the transverse distance from the center of the beam pipe to the vertex must be less than the radius of the beam pipe, which is approximately 2 cm. Finally, the uncertainty in the transverse distance between the beam axis and the vertex (d_{BV}), $\sigma_{d_{\mathrm{BV}}}$, must be < 25 μm. This criterion helps to reject vertices from decays of Lorentz-boosted particles, such as B mesons, which tend to have larger $\sigma_{d_{\mathrm{BV}}}$.

This search specifically targets events with at least one displaced vertex. The value of n_{track} serves as a discriminant between signal and background events. Vertices with n_{track} of at least five are considered as signal vertices, while vertices with n_{track} of three or four are used as control samples for background estimation. In cases where there are multiple displaced vertices, the one with the highest number of tracks is selected for signal extraction.

V. MACHINE LEARNING ALGORITHM

The vertex reconstruction and selection largely suppress backgrounds from SM LLPs, such as B and K mesons. The remaining background events are dominated by $t\bar{t}$ and QCD events, with background vertices originating from unrelated tracks that coincidentally overlap with each other. To further reduce such background vertices, the IN algorithm is used in this analysis. This section introduces the architecture, training and testing, and performance evaluation of the IN.

A. Interaction network description

An IN is a type of graph neural network [61] that takes graphs, a data structure that is composed of nodes and edges, as input. Nodes can be used to represent objects and edges can be used to represent relations between different nodes. With all of these features, INs are capable of calculating the interactions between different objects in a multibody system and thus predict the final states of all physical objects in the system. We apply an IN to the analysis of CMS events by treating each collision as a multibody interaction. The unique topology of LLP decays produces relationships between tracks that an IN can be trained to identify. In this analysis, we train an IN to calculate the relationships between tracks and learn that tracks resulting from LLP decays originate from displaced spatial points. As a result, the IN can output a discriminant

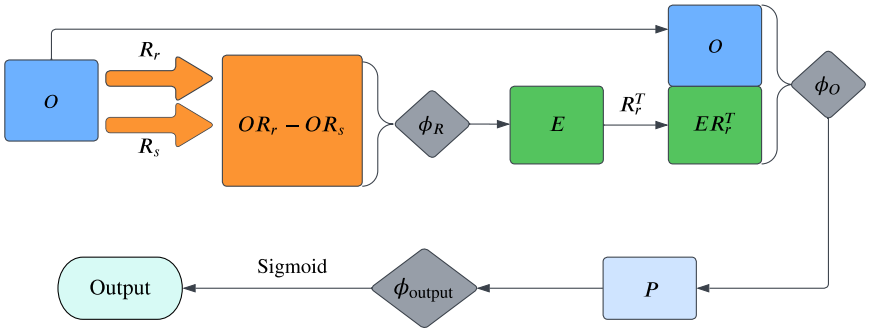

FIG. 2. An illustration of the architecture of the IN, where the flow of data is indicated by arrows. Rectangular boxes represent data matrices, while diamonds represent multilayer perceptrons (MLPs). The original input information (O) is integrated with relation matrices (R_r and R_s) to form a graph that captures interactions between tracks. This graph is subsequently processed by an MLP (ϕ_R) to compute the effect (E) of the interactions. The effect is then combined with R_r and merged with the original input O. To assess the influence (P) of the effect on the original information, it undergoes further processing via another MLP (ϕ_O). Finally, the influence is passed through an MLP (ϕ_{output}) and a sigmoid function to produce the final output.

value for assessing whether a given event contains LLP decays predicted in scenarios beyond the SM.

Given that variables associated with the vertex reconstruction are very powerful at discriminating signal and background, including those variables in the IN does not improve the discrimination of background events as the IN will mostly rely on the reconstructed vertices. To enable the IN to exploit as much additional information as possible, the IN is provided tracking information but no information about the reconstructed vertices themselves. This approach allows the IN to make use of the topologies of tracks in signal and background events without the help of the existing vertex reconstruction algorithm. The output of the IN is used together with variables from reconstructed vertices to improve the search sensitivity, as described in Sec. VI.

Since the IN is computationally intensive, for each event, only the first 50 p_T -ordered tracks are used as input. Tracks are required to satisfy the quality criteria but not the displacement criterion described in Sec. IV, a choice that provides the IN the opportunity to consider additional tracks from LLP decays whose trajectories coincide with the beam axis. For the split-SUSY signal model, the average number of tracks used by the IN that are assigned to reconstructed signal vertices typically ranges from 4 to 10, depending on mass splitting and gluino $c\tau$. In the IN, the input tracks are implemented as nodes in the graph while edges are composed of relations between any pairs of tracks. The tracking information used in the IN includes p_T, η, the azimuthal angle (ϕ), d_{xy} and its significance, and the longitudinal impact parameter d_z and its significance.

The IN is implemented using standard deep neural network building blocks, such as multilayer perceptrons (MLPs) [62] and matrix operations including addition, subtraction, multiplication, and concatenation. The input is constructed from several matrices: the variable matrix O, which contains track information; the send relation matrix R_s, which represents the interaction a track sends to other tracks; and the receive relation matrix R_r, which represents the interaction a track receives from other tracks. The interaction described in the IN is an abstract concept that could include any relationship between a pair of tracks.

Both R_r and R_s are structured such that each row represents a single track, and each column corresponds to the various interactions that tracks can send or receive. We want the IN to consider all possible relationships between tracks, so each element of R_r is set to zero or one such that every track can receive interactions from every track except itself, and each element of R_s is similarly set to zero or one such that every track can send interactions to every track except itself.

A diagram of the architecture of the IN is shown in Fig. 2. The IN calculates the state after tracks receive and send relations with other tracks by OR_r and OR_s, and combines these calculated elements together as a single matrix by $OR_r - OR_s$. The calculated matrix is passed into a five-layer MLP, labeled ϕ_R, with 50 nodes per layer. The matrix E, which is the output of ϕ_R, is interpreted as the effect of all relations having acted on each track. The effect on every track is represented as an array of length 20 in matrix E. The effect matrix E is multiplied with the transpose of matrix R_r to calculate the effect received by objects. The result is combined with the original variable matrix O to form a new matrix C, which contains the original information together with the effects having acted on tracks. The matrix C is processed by another MLP with two parts. The first part, labeled as ϕ_O, has two layers with 50 nodes in each layer and outputs matrix P. The second part, labeled as ϕ_{output}, has three layers with 100 nodes in each layer. It takes matrix P as input and outputs a vector that contains a single MLP output value for each event. Finally, this output value is processed with a sigmoid function to produce an IN output score (S_{ML}), which predicts whether an event contains an LLP decay or not.

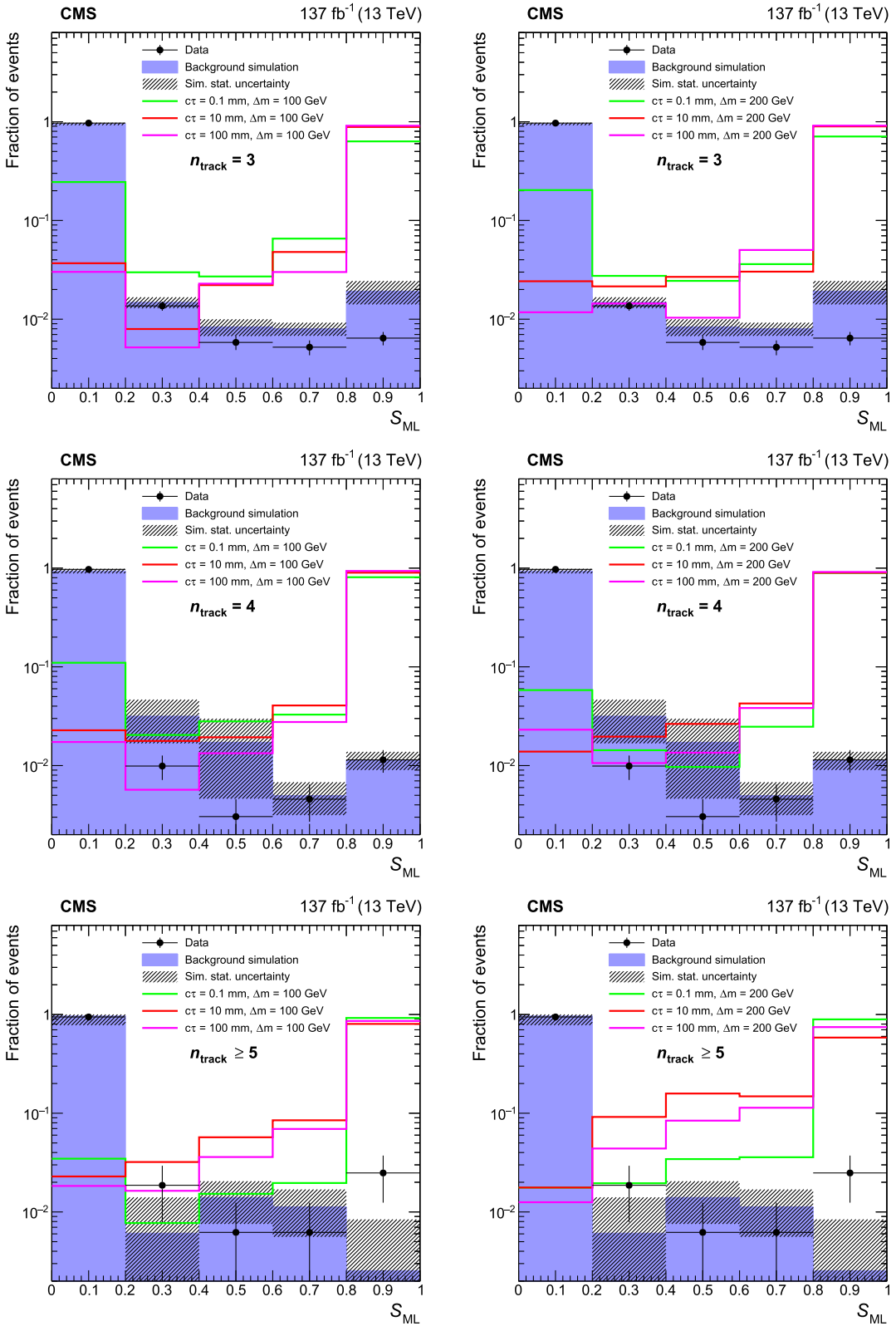

FIG. 3. Distributions of S_{ML} for data, simulated background, and signal. Events with n_{track} of 3 (upper), 4 (middle), and ≥ 5 (lower) are shown individually. The background simulation is shown for illustration and it is not used in the search. The distributions are shown for split-SUSY signals with a gluino mass of 2000 GeV and neutralino mass of 1900 GeV (left) and 1800 GeV (right). Different gluino proper decay lengths and mass difference between the gluino and neutralino, are shown as $c\tau$ and Δm in the legend. All distributions are normalized to unity.

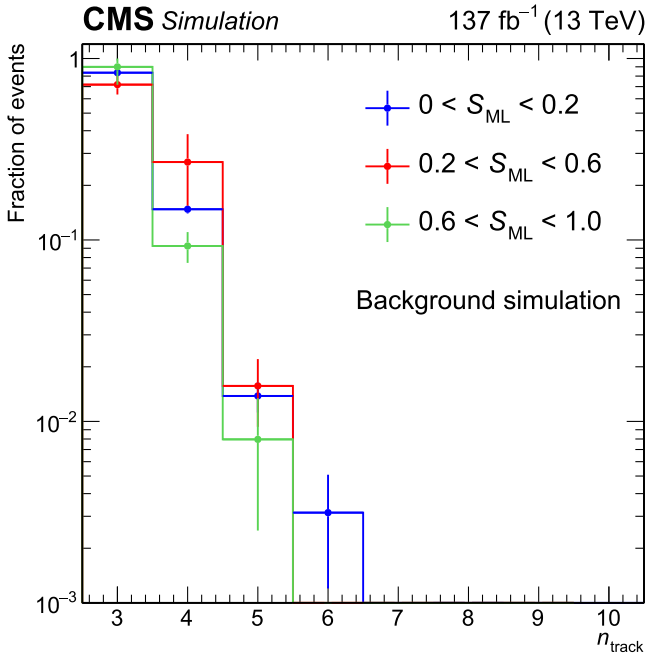

FIG. 4. The distribution of n_{track} in different S_{ML} regions for simulated background events. Events with $0 < S_{ML} < 0.2$ (blue), $0.2 < S_{ML} < 0.6$ (red), and $0.6 < S_{ML} < 1.0$ (green) are compared. All distributions are normalized to unity. The similar n_{track} distributions demonstrate that n_{track} and S_{ML} are decorrelated.

B. Training and testing

As a discriminant that predicts whether an event is signal or background, the S_{ML} is designed to have a value of 0 corresponding to background events and a value of 1 corresponding to signal events. The training process aims to optimize the discriminating power of the S_{ML}. The IN is trained by iteratively minimizing the loss function [63], which is composed of several parts: a binary cross entropy L_{bce} [63], an L2 regularization L_{reg} [64], and a distance correlation term L_{dcorr} [65]. The binary cross entropy L_{bce} is a commonly used metric for binary discriminant tasks. It quantifies the discrepancy between the predicted outcomes and the desired outcomes. The L2 regularization term L_{reg} is calculated as the sum of the squared magnitudes of the model parameters and serves to prevent overfitting by constraining these parameters. In background events, a distance correlation (DisCo) [66] method is used to decorrelate S_{ML} from n_{track} so that these two variables can be used in the background estimation method described in Sec. VII. The DisCo method adds L_{dcorr} to the IN loss function, which is based on the degree of correlation between S_{ML} and the n_{track} value of the vertex with the largest number of tracks in background events. We note that fewer than 0.05% of background events contain more than one reconstructed displaced vertex. The complete IN loss function is then $L = L_{bce} + \lambda_{reg} L_{reg} + \lambda_{dcorr} L_{dcorr}$, where λ_{reg} and λ_{dcorr} are hyperparameters that control the strength of each restriction. In each iteration, the IN processes all training sample events in batches of 128 events and updates the MLP parameters after processing each batch using the Adam algorithm [67] to minimize the loss function. Matrix elements of R_r and R_s are not updated during the training since they are just used to establish the relationships between tracks.

The events used for training, validation, and testing are required to have at least one reconstructed vertex with $n_{track} \geq 3$ and pass all event preselection requirements except the offline p_T^{miss} selection. Training and validation events are required to have $80 < p_T^{miss} < 200$ GeV to ensure orthogonality with testing events, which have $p_T^{miss} > 200$ GeV. Within the training and validation events, 85% of them are used for training, and 15% are used for validation. To avoid any bias introduced by potential mismodeling of simulated events, 17 067 data events and 31 165 simulated background events are mixed together and labeled as background events during the training of the IN. The simulated background events are drawn from different simulated SM processes in proportion to their cross section. To avoid potential bias, data events that include vertices with $n_{track} \geq 5$ are excluded from the training and validation samples. Split-SUSY signal samples with different lifetimes and masses are combined and labeled as signal events in the training, and events from different data-taking periods are combined during training. Specifically, 91 013 events are used for training and 17 065 events are used for validation.

Hyperparameter values are set to $\lambda_{reg} = 0.00005$ and $\lambda_{dcorr} = 0.65$, which ensures that the model is not overtrained and S_{ML} is uncorrelated with n_{track}. A learning rate of 0.0003 is chosen to avoid the case that the training does not converge because of a large learning rate. Models with different combinations of hyperparameters were tested, and the trained model that provides the best discriminating power while satisfying the decorrelation requirement between S_{ML} and n_{track} is used for all events in all data-taking periods.

C. Performance

The testing events are used to evaluate the performance of the IN. The S_{ML} distributions in simulated background events and split-SUSY signal events with $n_{track} = 3$, 4, and ≥ 5 are shown in Fig. 3. The significant differences between the S_{ML} distributions of background and signal samples show the strong discriminating power of the IN. Tagging events with $S_{ML} > 0.2$ as signal-like events correctly identifies approximately 97% of signal events while rejecting approximately 97% of background events.

The S_{ML} distributions of signal events with $n_{track} \geq 5$ have an increased likelihood around S_{ML} of 0.4 that is caused by the decorrelation term of the IN loss function. During the training, background events with larger n_{track} are more likely to obtain higher S_{ML} without the DisCo

regulation. To achieve the decorrelation, the IN tends to assign a smaller S_{ML} value to events with larger n_{track}. Given that events from signal samples with larger mass splittings and lifetimes are more likely to have well-reconstructed vertices with larger n_{track}, they are also more likely to obtain a smaller S_{ML}.

To estimate the effect of decorrelation between S_{ML} and n_{track}, we divide events into three regions depending on the S_{ML}: $0 < S_{\mathrm{ML}} < 0.2$, $0.2 < S_{\mathrm{ML}} < 0.6$, and $0.6 < S_{\mathrm{ML}} < 1.0$. The n_{track} distributions in different regions are compared, as shown in Fig. 4. As seen in the distributions, background events have similar n_{track} distributions in different S_{ML} regions, which demonstrates the success of the decorrelation technique.

VI. EVENT SELECTION AND SIGNAL EFFICIENCY

The signal region contains all events that pass the event preselection, have at least one displaced vertex with $n_{\mathrm{track}} \geq 5$, and have $S_{\mathrm{ML}} > 0.2$. The overall signal selection efficiency, which is defined as the fraction of generated signal events that pass the signal region selection, is directly related to the track reconstruction efficiency, vertex reconstruction efficiency, and ML tagging efficiency. It is important to understand these efficiencies in data and simulation and account for any observed differences. The procedures are based on methods similar to those of Ref. [24]. The simulated background processes described in Sec. III are used in the studies.

The track reconstruction efficiency is studied as a function of d_{BV} in data and simulation using events enriched in $K^0_S \to \pi^-\pi^+$ decays. The K^0_S decays are selected by requiring events that satisfy the preselection and contain a pair of tracks that form a well-reconstructed and displaced vertex. The vertex is required to be located inside the beam pipe, and the invariant mass of the two tracks associated with the vertex is required to be between 0.490 and 0.505 GeV when assuming the charged-π mass hypothesis. The d_{BV} distribution of resulting K^0_S vertices is compared between data and simulation to determine potential corrections to the signal simulation. The d_{BV} distribution in simulation is normalized such that the number of K^0_S vertices is consistent with data in the 0.5–0.8 mm region, where tracking efficiency is known to be well modeled and the number of K^0_S vertices results in a sufficiently small statistical uncertainty in the normalization. The number of reconstructed K^0_S vertices in data and simulation as a function of d_{BV} is shown in Fig. 5. Given that each K^0_S vertex is composed of two tracks and failing to reconstruct one track is the dominant cause of the failure to reconstruct a K^0_S vertex, the track reconstruction efficiency is proportional to the square root of the K^0_S vertex reconstruction efficiency. The ratio of data-to-simulation track reconstruction efficiency is found to be between 98 and 100% in all data-taking periods and bins of d_{BV}. These ratios are used to derive systematic uncertainties in the signal efficiency using the procedure described in Sec. VIII A.

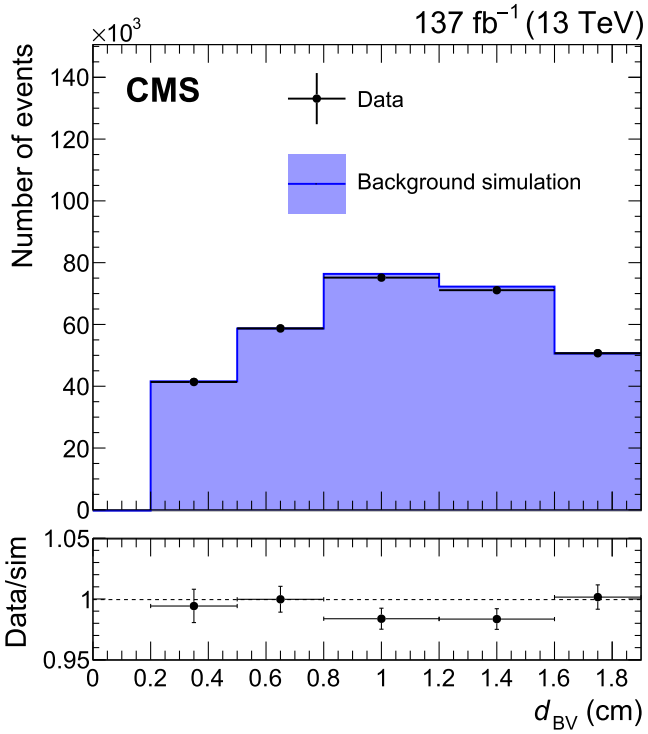

FIG. 5. The distribution of d_{BV} in K^0_S vertices in data (black) and simulation (purple). The lower panel shows the ratio between data and simulation.

The vertex reconstruction and ML tagging efficiencies are studied by artificially displacing tracks in data and simulated background events to produce displaced vertices that mimic displaced vertices generated by LLP decays in signal events. Events are required to satisfy the preselection, which results in a sample dominated by background processes because of the lack of track displacement and vertex reconstruction requirements. All simulated background processes described in Sec. III are used in the study. From the selected events, jets with $p_{\mathrm{T}} > 20$ GeV and at least three matched PF candidate tracks are considered for further study. These jets are categorized as b or light jets based on whether they pass or fail the "tight" working point of the DEEPJET algorithm [68], which has a b tagging efficiency of 55%–65% in QCD events with $p_{\mathrm{T}} > 30$ GeV and a misidentification rate for light jets of 0.1%. To mimic the topology of signal events, two light jets are randomly selected and tracks associated with the selected jets are displaced simultaneously from the primary vertex. The direction of the displacement is determined by the vector sum of the selected jet momenta, which is then subjected to a Gaussian smear with a standard deviation of 2.0 rad on both ϕ and the polar angle θ, while the magnitude of the displacement is randomly sampled from an exponential

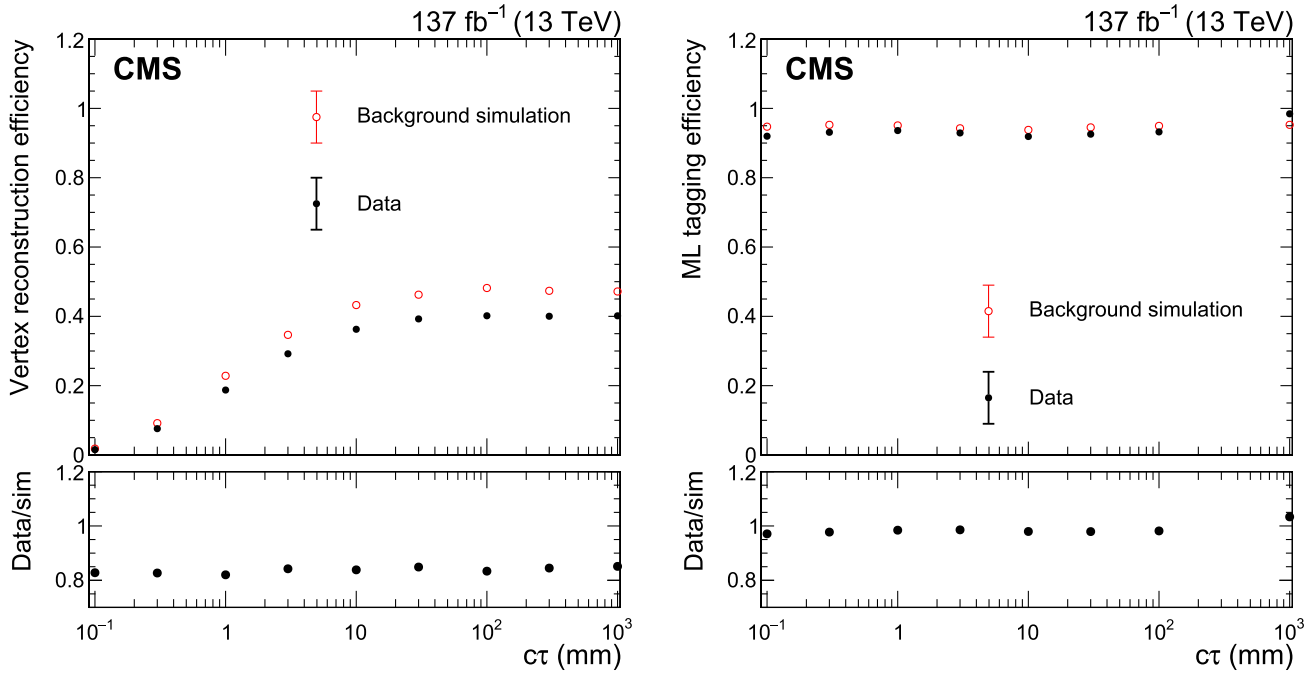

FIG. 6. The vertex reconstruction efficiency (left) and ML tagging efficiency (right) for artificially displaced vertices in data (black) and simulation (red). In this example, the artificially displaced vertices are corrected to mimic split-SUSY signal events with gluino mass of 2000 GeV and neutralino mass of 1800 GeV. The uncertainties are too small to be visible in the plot.

distribution with $c\tau$ of 10 mm, which reproduces the gluino decays in the simulated signal events. Corrections to the angular separation and the number of artificially displaced tracks per jet, derived from the ratios of those distributions between signal and events with artificial track displacements, are applied to ensure they describe signal vertices well.

The vertex reconstruction and ML algorithms are then applied to the events with artificially displaced tracks. The vertex reconstruction efficiency is calculated as the fraction of all artificially displaced vertices that are reconstructed within 200 μm of the expected position and satisfy the vertex selections described in Sec. IV. The ML tagging efficiency is calculated as the fraction of events with a reconstructed vertex that have S_{ML} larger than 0.2. The efficiencies are measured for both data and simulated events, and are compared in Fig. 6. The vertex reconstruction efficiency ratios between data and simulation range from 80% to 97%, depending on different mass splittings, while the ML tagging efficiency ratios range from 91% to 100% for different mass splittings. In contrast, the data-to-simulation efficiency ratios differ by less than a few percent between samples with different gluino masses and $c\tau$ values. Therefore, the efficiency ratio value used to calculate correction factors and systematic uncertainties is only dependent on the mass splitting and data-taking period.

The simulated signal event yield is corrected by scaling the vertex reconstruction efficiency ratio to reproduce the expected behavior in data. The differences between unity and the vertex efficiency and ML tagging efficiency ratios are used as systematic uncertainties following the procedures described in Sec. VIII.

VII. BACKGROUND ESTIMATION

The background events that pass the signal region selection are expected to be dominated by events in which displaced vertices are formed by random crossings of otherwise unrelated tracks. We estimate the number of such events and validate the estimation procedure using regions in data that are chosen to be orthogonal to the signal region and dominated by similar events. The control and validation regions are constructed from all events that pass the event preselection and have at least one reconstructed displaced vertex with $n_{\mathrm{track}} \geq 3$ but do not pass the signal region selections ($n_{\mathrm{track}} \geq 5$ and $S_{\mathrm{ML}} > 0.2$). Compared with background events in the signal region, background vertices with lower numbers of tracks are similar because they result from the same effect, i.e., unrelated tracks randomly crossing each other. However, the possibility to form a high track multiplicity background vertex is lower because it is less likely to have more tracks crossing the same spatial point by coincidence. The events passing these selections are then separated into three bins of n_{track} ($n_{\mathrm{track}} = 3$, 4, or ≥ 5), and each n_{track} bin is further divided into two bins depending on whether $S_{\mathrm{ML}} > 0.2$ is satisfied. Figure 7 illustrates how the control regions (labeled B, D, E, and F), validation region (C), and signal region (A) are arranged in the plane defined by n_{track} and

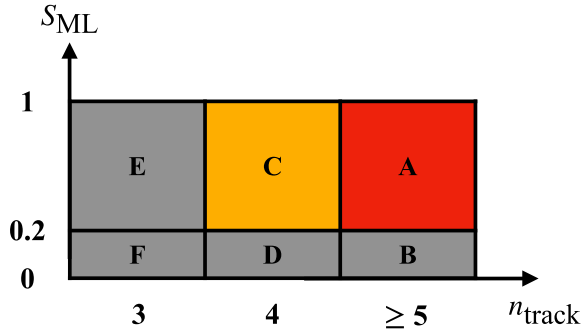

FIG. 7. A schematic diagram of the signal (red), validation (yellow), and control (gray) regions. The letter in each box corresponds to the region label described in the text.

S_{ML}. All control and validation regions are dominated by background events from $t\bar{t}$ and QCD processes.

The background estimation method takes advantage of the statistical independence of S_{ML} and n_{track}, which is ensured by the DisCo method. Because the fraction of background events that satisfy S_{ML} is independent of the value of n_{track}, the ratio of events in region E to events in region F should be consistent with the equivalent ratios of regions C to D and regions A to B, within the statistical uncertainty. The number of background events in the validation and signal regions can therefore be estimated as

$$N^{\mathrm{A}}_{\mathrm{bkg}} = \frac{N^{\mathrm{B}}_{\mathrm{bkg}} N^{\mathrm{E}}_{\mathrm{bkg}}}{N^{\mathrm{F}}_{\mathrm{bkg}}}, \tag{2}$$

$$N^{\mathrm{C}}_{\mathrm{bkg}} = \frac{N^{\mathrm{D}}_{\mathrm{bkg}} N^{\mathrm{E}}_{\mathrm{bkg}}}{N^{\mathrm{F}}_{\mathrm{bkg}}}. \tag{3}$$

To validate the background estimation procedure that is used to estimate the number of events in region A using Eq. (2), we predict the number of events in region C using Eq. (3) and compare this prediction to the observed number of events in region C. The prediction and observation agree within statistical uncertainties.

VIII. SYSTEMATIC UNCERTAINTIES

A. Systematic uncertainties affecting signal

Systematic uncertainties associated with signal reconstruction are due to uncertainties in the modeling of the track reconstruction efficiency, vertex reconstruction efficiency, ML tagging efficiency, $p_{\mathrm{T}}^{\mathrm{miss}}$, choice of PDF, trigger efficiency, pileup, integrated luminosity, and running conditions. The dominant source of systematic uncertainty is associated with the choice of PDF, followed by the modeling of vertex reconstruction efficiency.

The track reconstruction efficiency impacts the signal efficiency because $n_{\mathrm{track}} \geq 5$ is one of the signal region selections. In cases where an LLP decays to exactly five charged particles, failure to reconstruct even one of the five tracks will cause the vertex to fall outside of the signal region, and the impact of track reconstruction on such vertices is calculated as the fifth power of the track reconstruction efficiency. On the other hand, for vertices with more than five tracks, the failure to reconstruct any of the tracks will not necessarily cause the vertex to be excluded from the signal region, as long as there are at least five tracks remaining. Since the track reconstruction efficiency in data and simulation agree within 2%, the impact of track reconstruction efficiency is negligible for those vertices. We apply a systematic uncertainty equal to the differences in the fifth power of the track reconstruction efficiency observed in the study described in Sec. VI. The assigned uncertainties range from 6% to 21%, depending on signal mass, signal lifetime, and data-taking period.

In addition, a systematic uncertainty associated with the correction to the vertex reconstruction efficiency, described in Sec. VI, is assigned to account for the potential remaining differences between data and simulation, discrepancies between artificially displaced events and simulated signal events, differences between different gluino masses and proper decay lengths, and other small effects. The systematic uncertainties are taken to be the differences in vertex reconstruction efficiency between data and simulation observed in the study described in Sec. VI, with values ranging from 3% to 20%.

Similarly, a systematic uncertainty associated with ML tagging efficiency is assigned to account for any differences in the behavior of the ML algorithm between data and simulation. The magnitude of this uncertainty obtained as the difference of ML tagging efficiency between data and simulation in the study described in Sec. VI, ranges from negligibly small to 24%.

Potential mismodeling of jet and unclustered energy scales and jet energy corrections impact the $p_{\mathrm{T}}^{\mathrm{miss}}$ value, and therefore affect the $p_{\mathrm{T}}^{\mathrm{miss}}$ selection efficiency. To account for this effect, we assign a systematic uncertainty of up to 8%, derived from the change in signal efficiency when varying the parameters associated with the mismodeling by 1 standard deviation about their mean. The variations of the PDF could result in changes in the selection efficiency in the signal region. The associated uncertainty is evaluated by reweighting simulated signal events using the variation observed between NNPDF replica sets [69]. For most of the signal samples, the resulting PDF uncertainty is within 20%. However, for signal samples with very low signal efficiency, as the ones with mass splittings below 50 GeV and $c\tau$ values of 0.1 or 1000 mm, the PDF uncertainty is affected by statistical fluctuations and reaches values as large as 85%. The trigger efficiency systematic uncertainty is determined by its statistical uncertainty and the variation when using different data sets, resulting in an uncertainty of 1%–6%. The uncertainty associated with the modeling of the pileup distribution is 2%–15%. The integrated luminosity measurements for the 2016, 2017, and 2018

TABLE I. Summary of systematic uncertainties that affect the signal yield. The magnitude of each systematic varies by data-taking period and signal parameters, so a range of values is given in each case.

Systematic uncertainty	Magnitude (%)
Track reconstruction	6–21
Vertex reconstruction	3–20
ML tagging	$\lesssim 24$
$\vec{p}_{\mathrm{T}}^{\,\mathrm{miss}}$ selection	$\lesssim 8$
PDF uncertainty	1–85
Trigger efficiency	1–6
Pileup	2–15
Integrated luminosity	1–3
L1 trigger inefficiency	$\lesssim 1$
Total	8–91

data-taking years have 1%–3% individual uncertainties [70–72], while the overall uncertainty for the 2016–2018 period is 1.6%. During 2016 and 2017 data-taking periods, a gradual timing shift in the ECAL was not correctly accounted for in the L1 trigger, resulting in an efficiency drop for events with significant ECAL energy distributed in the high η region. This effect results in an uncertainty in the signal yield up to 1%.

A summary of systematic uncertainties that affect the signal yield is presented in Table I. The overall systematic uncertainty is calculated by summing individual components in quadrature under the assumption that there are no correlations between them.

B. Systematic uncertainties in background estimation

Since the background is estimated from data, potential mismodeling of the simulation does not have an impact. The number of events in the signal region is predicted using the number of events in control regions B, E, and F, which are based on 3-track and 5-track control regions. Given that the two variables that define the search regions are statistically independent, the prediction of the number of background events in the signal region based on Eq. (2) should be the same using 3-track control regions (E and F) or 4-track control regions (C and D). To validate this assumption, we compare two predictions of the number of background events in the signal region, one based on 3-track control regions and the other based on 4-track control regions. We find that the two predictions are compatible within the statistical uncertainty and therefore do not assign an additional systematic uncertainty in the background estimation.

TABLE II. Number of predicted and observed events in the control, validation, and search regions. Predictions are calculated using Eqs. (2) and (3) and fitting the data under the background-only hypothesis. Regions are organized by S_{ML} and n_{track} values, and region names corresponding to Fig. 7 are given in parentheses. The predicted number of events that pass the S_{ML} selection and the observed number of events that pass or fail the S_{ML} selection are shown in separate rows.

	$n_{\mathrm{track}} = 3$	$n_{\mathrm{track}} = 4$	$n_{\mathrm{track}} \geq 5$
Predicted $S_{\mathrm{ML}} > 0.2$	⋯ (E)	38.0 ± 6.0 (C)	5.2 ± 0.5 (A)
Observed $S_{\mathrm{ML}} > 0.2$	203 (E)	38 (C)	9 (A)
Observed $S_{\mathrm{ML}} < 0.2$	6327 (F)	1276 (D)	152 (B)

IX. RESULTS AND STATISTICAL INTERPRETATION

A maximum likelihood fit under the background-only hypothesis is performed on all search regions. Systematic uncertainties described in Sec. VIII are taken to be uncorrelated and used as nuisance parameters in the fit. The predicted and observed numbers of events in all search regions after the fit are reported in Table II. In the signal region, nine events are observed while 5.2 ± 0.5 events are predicted, which corresponds to a p-value of 0.089. No significant discrepancy between the background-only fit prediction and the observation is seen.

Based on the observed number of events and the background prediction, constraints are set on parameters of the benchmark signal samples used in the search. Specifically, the 95% confidence level (CL) upper limit on the product of the production cross section and the square of the branching fraction ($\sigma\mathcal{B}^2$) of the decay mode is estimated using the $\mathrm{CL_s}$ method [73–75]. The signal yields are determined from simulated signal events, with all the corrections applied; the number of background events is determined purely from data. Datasets from different data-taking periods are treated separately and combined during the final fit. The upper limits are compared with the theoretical prediction of the production cross section and uncertainty [76] calculated at NNLO + NNLL precision [47] to exclude regions of the parameter space of the benchmark signal models. The branching fraction for the gluino decay to the targeted final state in split SUSY and GMSB SUSY is assumed to be 100% for all signal samples.

Figure 8 shows the upper limits and exclusion curves for the split-SUSY model as a function of gluino mass, gluino $c\tau$, and gluino-neutralino mass splitting. The search is most sensitive when gluino $c\tau$ is approximately 10 mm and the gluino-neutralino mass splitting is large, but the sensitivity extends to gluino $c\tau$ values from 0.1 to 1000 mm and mass splittings as low as 20 GeV. The decreasing sensitivity at the low $c\tau$ values is driven by the decreasing displaced vertex reconstruction efficiency, while the decreasing sensitivity at highest $c\tau$ values is driven by the constraint that the displaced vertex must be within the CMS beam pipe. Figure 9 shows the upper limits and exclusion curves for the GMSB SUSY model as a function of gluino mass and $c\tau$, which exhibit a similar dependence on gluino lifetime to those associated with the split-SUSY model.

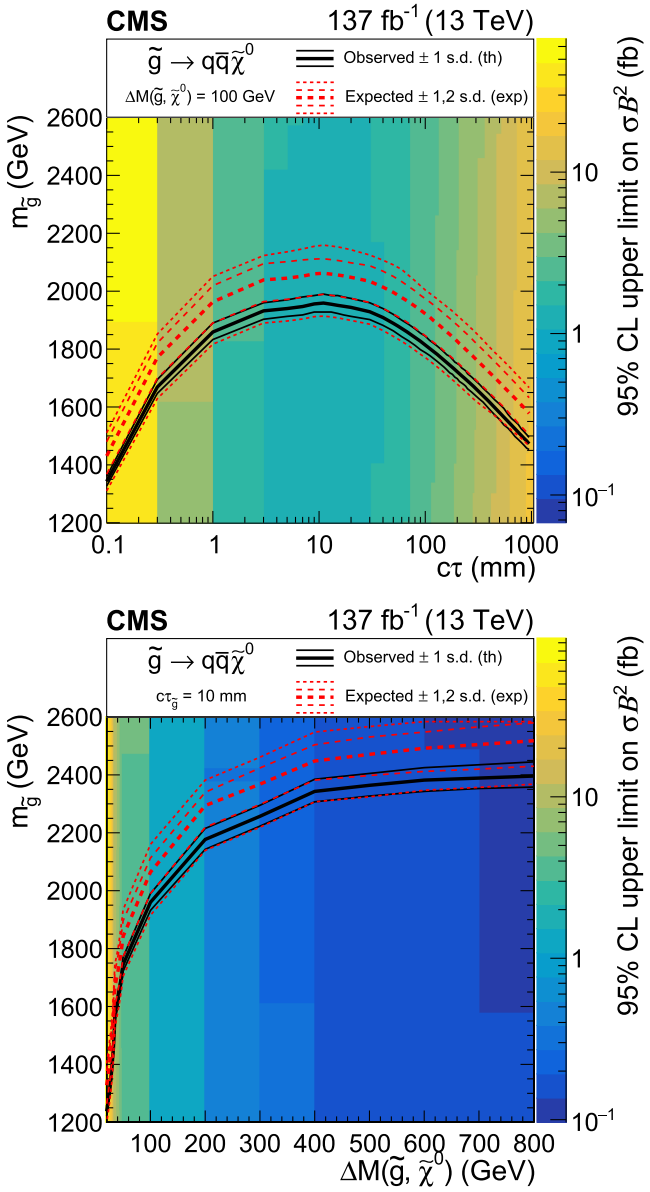

FIG. 8. Upper: the 95% CL_s upper limit on the product of the cross section and branching fraction squared for the split-SUSY signal model with a mass splitting of 100 GeV, shown as a function of gluino mass and $c\tau$. Lower: the 95% CL_s upper limit on the product of the cross section and branching fraction squared for the split-SUSY model with a $c\tau$ of 10 mm, shown as a function of gluino mass and mass splitting. For both plots, the observed (solid black) and expected (dashed red) exclusion curves are shown.

The observed upper limits are weaker than the expected by about 1.35 standard deviations since more events are observed in the signal region compared to the expectation. As this search uses only one signal region, the upper limits for different signal parameters are calculated using the same region, which makes the difference between observed and expected upper limits similar for different signal parameters. For the split-SUSY benchmark signal model,

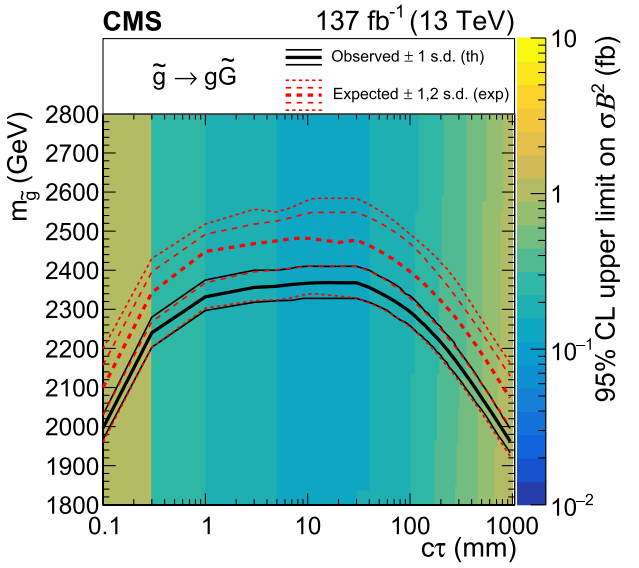

FIG. 9. The 95% CL_s upper limit on the product of the cross section and branching fraction squared for the GMSB SUSY signal model, shown as a function of gluino mass and $c\tau$. The observed (solid black) and expected (dashed red) exclusion curves are shown.

the search excludes gluinos with $c\tau$ in the range 1–100 mm and masses below 1800 GeV for mass splittings of 100 GeV with respect to the neutralino. Also, for mass splittings above 50 GeV, the search excludes gluinos with masses below 1600 GeV and $c\tau$ between 1–30 mm. For gluino masses of 1400 GeV and neutralino masses of 1300 GeV, this search excludes production cross sections that are a factor of 2–100 times smaller than those excluded by Ref. [22] and 10–100 times smaller than those excluded by Ref. [29], depending on the gluino lifetime. For the GMSB SUSY signal model, the search achieves upper limits on the product of the cross section and branching fraction squared as low as 1 fb for gluinos with $c\tau$ ranging from 0.1 to 1000 mm and excludes gluinos with $c\tau$ in the range 0.3–100 mm and masses below 2240 GeV.

X. SUMMARY

A search for the production of long-lived particles that decay to at least one displaced vertex with missing transverse momentum in proton-proton collisions at a center-of-mass energy of 13 TeV collected by the CMS detector has been presented. The analysis extends the previous CMS search [24] by improving the sensitivity to events with low total jet energy, targeting events with as few as one displaced vertex, and introducing a dedicated machine learning algorithm that reduces the number of background events in the signal region by 94%. Split supersymmetry (SUSY) and gauge-mediated SUSY breaking are used as benchmark signal models for statistical interpretations in this search.

At 95% confidence level, the search excludes long-lived gluinos predicted by the split-SUSY model with masses below 1800 GeV and mean proper decay lengths in the range of 1 to 100 mm, when the mass splitting is 100 GeV. For mass splittings above 50 GeV, gluinos with masses below 1600 GeV and mean proper decay lengths between 1 and 30 mm are excluded. For the gauge-mediated SUSY breaking model, gluinos with masses below 2200 GeV and mean proper decay lengths between 0.3 and 100 mm are excluded. This search is the first CMS search that shows sensitivity to hadronically decaying long-lived particles from signals with mass differences between the gluino and neutralino below 100 GeV. It sets the most stringent limits to date for split-SUSY models and for GMSB gluinos with proper decay length less than 6 mm.

ACKNOWLEDGMENTS

We congratulate our colleagues in the CERN accelerator departments for the excellent performance of the LHC and thank the technical and administrative staffs at CERN and at other CMS institutes for their contributions to the success of the CMS effort. In addition, we gratefully acknowledge the computing centers and personnel of the Worldwide LHC Computing Grid and other centers for delivering so effectively the computing infrastructure essential to our analyses. Finally, we acknowledge the enduring support for the construction and operation of the LHC, the CMS detector, and the supporting computing infrastructure provided by the following funding agencies: SC (Armenia), BMBWF and FWF (Austria); FNRS and FWO (Belgium); CNPq, CAPES, FAPERJ, FAPERGS, and FAPESP (Brazil); MES and BNSF (Bulgaria); CERN; CAS, MoST, and NSFC (China); MINCIENCIAS (Colombia); MSES and CSF (Croatia); RIF (Cyprus); SENESCYT (Ecuador); ERC PRG, RVTT3 and MoER TK202 (Estonia); Academy of Finland, MEC, and HIP (Finland); CEA and CNRS/IN2P3 (France); SRNSF (Georgia); BMBF, DFG, and HGF (Germany); GSRI (Greece); NKFIH (Hungary); DAE and DST (India); IPM (Iran); SFI (Ireland); INFN (Italy); MSIP and NRF (Republic of Korea); MES (Latvia); LMTLT (Lithuania); MOE and UM (Malaysia); BUAP, CINVESTAV, CONACYT, LNS, SEP, and UASLP-FAI (Mexico); MOS (Montenegro); MBIE (New Zealand); PAEC (Pakistan); MES and NSC (Poland); FCT (Portugal); MESTD (Serbia); MCIN/AEI and PCTI (Spain); MOSTR (Sri Lanka); Swiss Funding Agencies (Switzerland); MST (Taipei); MHESI and NSTDA (Thailand); TUBITAK and TENMAK (Turkey); NASU (Ukraine); STFC (United Kingdom); DOE and NSF (USA). Individuals have received support from the Marie-Curie program and the European Research Council and Horizon 2020 Grant, Contracts No. 675440, No. 724704, No. 752730, No. 758316, No. 765710, No. 824093, No. 101115353, and COST Action CA16108 (European Union); the Leventis Foundation; the Alfred P. Sloan Foundation; the Alexander von Humboldt Foundation; the Science Committee, Project No. 22rl-037 (Armenia); the Belgian Federal Science Policy Office; the Fonds pour la Formation *à la* Recherche dans l'Industrie et dans l'Agriculture (FRIA-Belgium); the Agentschap voor Innovatie door Wetenschap en Technologie (IWT-Belgium); the F. R. S.-FNRS and FWO (Belgium) under the "Excellence of Science—EOS"—be.h Project No. 30820817; the Beijing Municipal Science and Technology Commission, Grant No. Z191100007219010 and Fundamental Research Funds for the Central Universities (China); the Ministry of Education, Youth and Sports (MEYS) of the Czech Republic; the Shota Rustaveli National Science Foundation, Grant No. FR-22-985 (Georgia); the Deutsche Forschungsgemeinschaft (DFG), under Germany's Excellence Strategy—EXC 2121 "Quantum Universe"—Grant No. 390833306, and under Project No. 400140256—GRK2497; the Hellenic Foundation for Research and Innovation (HFRI), Project No. 2288 (Greece); the Hungarian Academy of Sciences, the New National Excellence Program—ÚNKP, the NKFIH Research Grants No. K 124845, No. K 124850, No. K 128713, No. K 128786, No. K 129058, No. K 131991, No. K 133046, No. K 138136, No. K 143460, No. K 143477, No. 2020-2.2.1-ED-2021-00181, and No. TKP2021-NKTA-64 (Hungary); the Council of Science and Industrial Research, India; ICSC—National Research Center for High Performance Computing, Big Data and Quantum Computing, funded by the NextGenerationEU program (Italy); the Latvian Council of Science; the Ministry of Education and Science, Project No. 2022/WK/14, and the National Science Center, contracts Opus No. 2021/41/B/ST2/01369 and No. 2021/43/B/ST2/01552 (Poland); the Fundação para a Ciência e a Tecnologia, Grant No. CEECIND/01334/2018 (Portugal); the National Priorities Research Program by Qatar National Research Fund; MCIN/AEI/10.13039/501100011033, ERDF "a way of making Europe", and the Programa Estatal de Fomento de la Investigación Científica y Técnica de Excelencia María de Maeztu, Grant No. MDM-2017-0765 and Programa Severo Ochoa del Principado de Asturias (Spain); the Chulalongkorn Academic into Its 2nd Century Project Advancement Project, and the National Science, Research and Innovation Fund via the Program Management Unit for Human Resources and Institutional Development, Research and Innovation, Grant No. B37G660013 (Thailand); the Kavli Foundation; the Nvidia Corporation; the SuperMicro Corporation; the Welch Foundation, Contract No. C-1845; and the Weston Havens Foundation (USA).

[1] G. F. Giudice and A. Romanino, Split supersymmetry, Nucl. Phys. **B699**, 65 (2004); **706**, 487(E) (2005).

[2] J. L. Hewett, B. Lillie, M. Masip, and T. G. Rizzo, Signatures of long-lived gluinos in split supersymmetry, J. High Energy Phys. 09 (2004) 070.

[3] N. Arkani-Hamed, S. Dimopoulos, G. F. Giudice, and A. Romanino, Aspects of split supersymmetry, Nucl. Phys. **B709**, 3 (2005).

[4] P. Gambino, G. F. Giudice, and P. Slavich, Gluino decays in split supersymmetry, Nucl. Phys. **B726**, 35 (2005).

[5] A. Arvanitaki, N. Craig, S. Dimopoulos, and G. Villadoro, Mini-split, J. High Energy Phys. 02 (2013) 126.

[6] N. Arkani-Hamed, A. Gupta, D. E. Kaplan, N. Weiner, and T. Zorawski, Simply unnatural supersymmetry, arXiv:1212.6971.

[7] P. Fayet, Supergauge invariant extension of the Higgs mechanism and a model for the electron and its neutrino, Nucl. Phys. **B90**, 104 (1975).

[8] G. R. Farrar and P. Fayet, Phenomenology of the production, decay, and detection of new hadronic states associated with supersymmetry, Phys. Lett. **76B**, 575 (1978).

[9] S. Weinberg, Supersymmetry at ordinary energies. Masses and conservation laws, Phys. Rev. D **26**, 287 (1982).

[10] R. Barbier, C. Bérat, M. Besançon, M. Chemtob, A. Deandrea, E. Dudas, P. Fayet, S. Lavignac, G. Moreau, E. Perez, and Y. Sirois, *R*-parity violating supersymmetry, Phys. Rep. **420**, 1 (2005).

[11] G. F. Giudice and R. Rattazzi, Theories with gauge mediated supersymmetry breaking, Phys. Rep. **322**, 419 (1999).

[12] P. Meade, N. Seiberg, and D. Shih, General gauge mediation, Prog. Theor. Phys. Suppl. **177**, 143 (2009).

[13] M. Buican, P. Meade, N. Seiberg, and D. Shih, Exploring general gauge mediation, J. High Energy Phys. 03 (2009) 016.

[14] J. Fan, M. Reece, and J. T. Ruderman, Stealth supersymmetry, J. High Energy Phys. 11 (2011) 012.

[15] J. Fan, M. Reece, and J. T. Ruderman, A stealth supersymmetry sampler, J. High Energy Phys. 07 (2012) 196.

[16] M. J. Strassler and K. M. Zurek, Echoes of a hidden valley at hadron colliders, Phys. Lett. B **651**, 374 (2007).

[17] M. J. Strassler and K. M. Zurek, Discovering the Higgs through highly-displaced vertices, Phys. Lett. B **661**, 263 (2008).

[18] T. Han, Z. Si, K. M. Zurek, and M. J. Strassler, Phenomenology of hidden valleys at hadron colliders, J. High Energy Phys. 07 (2008) 008.

[19] Z. Chacko, H.-S. Goh, and R. Harnik, Natural electroweak breaking from a mirror symmetry, Phys. Rev. Lett. **96**, 231802 (2006).

[20] D. Curtin and C. B. Verhaaren, Discovering uncolored naturalness in exotic Higgs decays, J. High Energy Phys. 12 (2015) 072.

[21] H.-C. Cheng, S. Jung, E. Salvioni, and Y. Tsai, Exotic quarks in twin Higgs models, J. High Energy Phys. 03 (2016) 074.

[22] ATLAS Collaboration, Search for long-lived, massive particles in events with displaced vertices and missing transverse momentum in $\sqrt{s} = 13$ TeV pp collisions with the ATLAS detector, Phys. Rev. D **97**, 052012 (2018).

[23] ATLAS Collaboration, Search for long-lived, massive particles in events with a displaced vertex and a muon with large impact parameter in pp collisions at $\sqrt{s} = 13$ TeV with the ATLAS detector, Phys. Rev. D **102**, 032006 (2020).

[24] CMS Collaboration, Search for long-lived particles decaying to jets with displaced vertices in proton-proton collisions at $\sqrt{s} = 13$ TeV, Phys. Rev. D **104**, 052011 (2021).

[25] CMS Collaboration, Search for long-lived particles using displaced jets in proton-proton collisions at $\sqrt{s} = 13$ TeV, Phys. Rev. D **104**, 012015 (2021).

[26] ATLAS Collaboration, Search for long-lived, massive particles in events with displaced vertices and multiple jets in pp collisions at $\sqrt{s} = 13$ TeV with the ATLAS detector, J. High Energy Phys. 06 (2023) 200.

[27] E. A. Moreno, O. Cerri, J. M. Duarte, H. B. Newman, T. Q. Nguyen, A. Periwal, M. Pierini, A. Serikova, M. Spiropulu, and J.-R. Vlimant, JEDI-net: A jet identification algorithm based on interaction networks, Eur. Phys. J. C **80**, 58 (2020).

[28] E. A. Moreno, T. Q. Nguyen, J.-R. Vlimant, O. Cerri, H. B. Newman, A. Periwal, M. Spiropulu, J. M. Duarte, and M. Pierini, Interaction networks for the identification of boosted $H \to b\bar{b}$ decays, Phys. Rev. D **102**, 012010 (2020).

[29] CMS Collaboration, Search for natural and split supersymmetry in proton-proton collisions at $\sqrt{s} = 13$ TeV in final states with jets and missing transverse momentum, J. High Energy Phys. 05 (2018) 025.

[30] HEPData record for this analysis (2024), 10.17182/hepdata.147272.

[31] CMS Collaboration, The CMS experiment at the CERN LHC, J. Instrum. **3**, S08004 (2008).

[32] CMS Collaboration, Description and performance of track and primary-vertex reconstruction with the CMS tracker, J. Instrum. **9**, P10009 (2014).

[33] W. Adam *et al.* (Tracker Group of the CMS), The CMS Phase-1 pixel detector upgrade, J. Instrum. **16**, P02027 (2021).

[34] CMS Collaboration, Track impact parameter resolution for the full pseudo rapidity coverage in the 2017 dataset with the CMS Phase-1 Pixel detector, CMS Detector Performance Summary, Report No. CMS-DP-2020-049, 2020, https://cds.cern.ch/record/2743740.

[35] CMS Collaboration, Particle-flow reconstruction and global event description with the CMS detector, J. Instrum. **12**, P10003 (2017).

[36] CMS Collaboration, Technical proposal for the Phase-II upgrade of the Compact Muon Solenoid, CMS Technical Proposal, Reports No. CERN-LHCC-2015-010, No. CMS-TDR-15-02, 2015, 10.17181/CERN.VU8I.D59J.

[37] M. Cacciari, G. P. Salam, and G. Soyez, The anti-k_T jet clustering algorithm, J. High Energy Phys. 04 (2008) 063.

[38] M. Cacciari, G. P. Salam, and G. Soyez, FastJet user manual, Eur. Phys. J. C **72**, 1896 (2012).

[39] CMS Collaboration, Jet energy scale and resolution in the CMS experiment in pp collisions at 8 TeV, J. Instrum. **12**, P02014 (2017).

[40] CMS Collaboration, CMS Jet algorithms performance in 13 TeV data, CMS Physics Analysis Summary, Report No. CMS-PAS-JME-16-003, 2016, https://cdsweb.cern.ch/record/2256875.
[41] CMS Collaboration, Performance of missing transverse momentum reconstruction in proton-proton collisions at $\sqrt{s} = 13$ TeV using the CMS detector, J. Instrum. **14**, P07004 (2019).
[42] CMS Collaboration, Performance of the CMS Level-1 trigger in proton-proton collisions at $\sqrt{s} = 13$ TeV, J. Instrum. **15**, P10017 (2020).
[43] CMS Collaboration, The CMS trigger system, J. Instrum. **12**, P01020 (2017).
[44] T. Sjöstrand, S. Ask, J. R. Christiansen, R. Corke, N. Desai, P. Ilten, S. Mrenna, S. Prestel, C. O. Rasmussen, and P. Z. Skands, An introduction to PYTHIA 8.2, Comput. Phys. Commun. **191**, 159 (2015).
[45] CMS Collaboration, Extraction and validation of a new set of CMS PYTHIA8 tunes from underlying-event measurements, Eur. Phys. J. C **80**, 4 (2020).
[46] R. D. Ball *et al.* (NNPDF Collaboration), Parton distributions from high-precision collider data, Eur. Phys. J. C **77**, 663 (2017).
[47] W. Beenakker, C. Borschensky, M. Krämer, A. Kulesza, and E. Laenen, NNLL-fast: Predictions for coloured supersymmetric particle production at the LHC with threshold and Coulomb resummation, J. High Energy Phys. 12 (2016) 133.
[48] J. Alwall, R. Frederix, S. Frixione, V. Hirschi, F. Maltoni, O. Mattelaer, H. S. Shao, T. Stelzer, P. Torrielli, and M. Zaro, The automated computation of tree-level and next-to-leading order differential cross sections, and their matching to parton shower simulations, J. High Energy Phys. 07 (2014) 079.
[49] J. Alwall, S. Höche, F. Krauss, N. Lavesson, L. Lönnblad, F. Maltoni, M. L. Mangano, M. Moretti, C. G. Papadopoulos, F. Piccinini, S. Schumann, M. Treccani, J. Winter, and M. Worek, Comparative study of various algorithms for the merging of parton showers and matrix elements in hadronic collisions, Eur. Phys. J. C **53**, 473 (2008).
[50] R. Frederix and S. Frixione, Merging meets matching in MC@NLO, J. High Energy Phys. 12 (2012) 061.
[51] P. Nason, A new method for combining NLO QCD with shower Monte Carlo algorithms, J. High Energy Phys. 11 (2004) 040.
[52] S. Frixione, P. Nason, and C. Oleari, Matching NLO QCD computations with parton shower simulations: The POWHEG method, J. High Energy Phys. 11 (2007) 070.
[53] S. Alioli, P. Nason, C. Oleari, and E. Re, A general framework for implementing NLO calculations in shower Monte Carlo programs: The POWHEG BOX, J. High Energy Phys. 06 (2010) 043.
[54] E. Re, Single-top *Wt*-channel production matched with parton showers using the POWHEG method, Eur. Phys. J. C **71**, 1547 (2011).
[55] S. Alioli, P. Nason, C. Oleari, and E. Re, NLO single-top production matched with shower in POWHEG: *s*- and *t*-channel contributions, J. High Energy Phys. 09 (2009) 111; 02 (2010) 11.
[56] R. D. Ball *et al.* (NNPDF Collaboration), Parton distributions for the LHC Run II, J. High Energy Phys. 04 (2015) 040.
[57] S. Agostinelli *et al.* (GEANT4 Collaboration), GEANT4—a simulation toolkit, Nucl. Instrum. Methods Phys. Res., Sect. A **506**, 250 (2003).
[58] R. Frühwirth, Application of Kalman filtering to track and vertex fitting, Nucl. Instrum. Methods Phys. Res., Sect. A **262**, 444 (1987).
[59] P. Billoir and S. Qian, Simultaneous pattern recognition and track fitting by the Kalman filtering method, Nucl. Instrum. Methods Phys. Res., Sect. A **294**, 219 (1990).
[60] P. Billoir and S. Qian, Further test for the simultaneous pattern recognition and track fitting by the Kalman filtering method, Nucl. Instrum. Methods Phys. Res., Sect. A **295**, 492 (1990).
[61] J. Zhou, G. Cui, S. Hu, Z. Zhang, C. Yang, Z. Liu, L. Wang, C. Li, and M. Sun, Graph neural networks: A review of methods and applications, AI Open **1**, 57 (2020).
[62] F. Murtagh, Multilayer perceptrons for classification and regression, Neurocomputing;Variable Star Bulletin **2**, 183 (1991).
[63] T. Gneiting and A. E. Raftery, Strictly proper scoring rules, prediction, and estimation, J. Am. Stat. Assoc. **102**, 359 (2007).
[64] A. Y. Ng, Feature selection, L1 vs. L2 regularization, and rotational invariance, in *Proceedings of the Twenty-First International Conference on Machine Learning* (2004), p. 78, 10.1145/1015330.1015435.
[65] G. Kasieczka and D. Shih, Robust jet classifiers through distance correlation, Phys. Rev. Lett. **125**, 122001 (2020).
[66] G. Kasieczka, B. Nachman, M. D. Schwartz, and D. Shih, Automating the ABCD method with machine learning, Phys. Rev. D **103**, 035021 (2021).
[67] D. P. Kingma and J. Ba, Adam: A method for stochastic optimization, arXiv:1412.6980.
[68] E. Bols, J. Kieseler, M. Verzetti, M. Stoye, and A. Stakia, Jet flavour classification using DeepJet, J. Instrum. **15**, P12012 (2020).
[69] J. Butterworth *et al.*, PDF4LHC recommendations for LHC Run II, J. Phys. G **43**, 023001 (2016).
[70] CMS Collaboration, Precision luminosity measurement in proton-proton collisions at $\sqrt{s} = 13$ TeV in 2015 and 2016 at CMS, Eur. Phys. J. C **81**, 800 (2021).
[71] CMS Collaboration, CMS luminosity measurement for the 2017 data-taking period at $\sqrt{s} = 13$ TeV, CMS Physics Analysis Summary, Report No. CMS-PAS-LUM-17-004, 2018, https://cds.cern.ch/record/2621960/.
[72] CMS Collaboration, CMS luminosity measurement for the 2018 data-taking period at $\sqrt{s} = 13$ TeV, CMS Physics Analysis Summary, Report No. CMS-PAS-LUM-18-002, 2019, https://cds.cern.ch/record/2676164/.
[73] A. L. Read, Presentation of search results: The CL_s technique, J. Phys. G **28**, 2693 (2002).

[74] T. Junk, Confidence level computation for combining searches with small statistics, Nucl. Instrum. Methods Phys. Res., Sect. A **434**, 435 (1999).
[75] CMS Collaboration, The CMS statistical analysis and combination tool: COMBINE, arXiv:2404.06614.
[76] C. Borschensky, M. Krämer, A. Kulesza, M. Mangano, S. Padhi, T. Plehn, and X. Portell, Squark and gluino production cross sections in pp collisions at $\sqrt{s} = 13$, 14, 33 and 100 TeV, Eur. Phys. J. C **74**, 3174 (2014).

A. Hayrapetyan,[1] A. Tumasyan,[1,b] W. Adam,[2] J. W. Andrejkovic,[2] T. Bergauer,[2] S. Chatterjee,[2] K. Damanakis,[2] M. Dragicevic,[2] P. S. Hussain,[2] M. Jeitler,[2,c] N. Krammer,[2] A. Li,[2] D. Liko,[2] I. Mikulec,[2] J. Schieck,[2,c] R. Schöfbeck,[2] D. Schwarz,[2] M. Sonawane,[2] S. Templ,[2] W. Waltenberger,[2] C.-E. Wulz,[2,c] M. R. Darwish,[3,d] T. Janssen,[3] P. Van Mechelen,[3] E. S. Bols,[4] J. D'Hondt,[4] S. Dansana,[4] A. De Moor,[4] M. Delcourt,[4] S. Lowette,[4] I. Makarenko,[4] D. Müller,[4] S. Tavernier,[4] M. Tytgat,[4,e] G. P. Van Onsem,[4] S. Van Putte,[4] D. Vannerom,[4] B. Clerbaux,[5] A. K. Das,[5] G. De Lentdecker,[5] H. Evard,[5] L. Favart,[5] P. Gianneios,[5] D. Hohov,[5] J. Jaramillo,[5] A. Khalilzadeh,[5] F. A. Khan,[5] K. Lee,[5] M. Mahdavikhorrami,[5] A. Malara,[5] S. Paredes,[5] L. Thomas,[5] M. Vanden Bemden,[5] C. Vander Velde,[5] P. Vanlaer,[5] M. De Coen,[6] D. Dobur,[6] Y. Hong,[6] J. Knolle,[6] L. Lambrecht,[6] G. Mestdach,[6] K. Mota Amarilo,[6] C. Rendón,[6] A. Samalan,[6] K. Skovpen,[6] N. Van Den Bossche,[6] J. van der Linden,[6] L. Wezenbeek,[6] A. Benecke,[7] A. Bethani,[7] G. Bruno,[7] C. Caputo,[7] C. Delaere,[7] I. S. Donertas,[7] A. Giammanco,[7] Sa. Jain,[7] V. Lemaitre,[7] J. Lidrych,[7] P. Mastrapasqua,[7] T. T. Tran,[7] S. Wertz,[7] G. A. Alves,[8] E. Coelho,[8] C. Hensel,[8] T. Menezes De Oliveira,[8] A. Moraes,[8] P. Rebello Teles,[8] M. Soeiro,[8] W. L. Aldá Júnior,[9] M. Alves Gallo Pereira,[9] M. Barroso Ferreira Filho,[9] H. Brandao Malbouisson,[9] W. Carvalho,[9] J. Chinellato,[9,f] E. M. Da Costa,[9] G. G. Da Silveira,[9,g] D. De Jesus Damiao,[9] S. Fonseca De Souza,[9] R. Gomes De Souza,[9] J. Martins,[9,h] C. Mora Herrera,[9] L. Mundim,[9] H. Nogima,[9] J. P. Pinheiro,[9] A. Santoro,[9] A. Sznajder,[9] M. Thiel,[9] A. Vilela Pereira,[9] C. A. Bernardes,[10,g] L. Calligaris,[10] T. R. Fernandez Perez Tomei,[10] E. M. Gregores,[10] P. G. Mercadante,[10] S. F. Novaes,[10] B. Orzari,[10] Sandra S. Padula,[10] A. Aleksandrov,[11] G. Antchev,[11] R. Hadjiiska,[11] P. Iaydjiev,[11] M. Misheva,[11] M. Shopova,[11] G. Sultanov,[11] A. Dimitrov,[12] L. Litov,[12] B. Pavlov,[12] P. Petkov,[12] A. Petrov,[12] E. Shumka,[12] S. Keshri,[13] S. Thakur,[13] T. Cheng,[14] T. Javaid,[14] L. Yuan,[14] Z. Hu,[15] J. Liu,[15] K. Yi,[15,i,j] G. M. Chen,[16,k] H. S. Chen,[16,k] M. Chen,[16,k] F. Iemmi,[16] C. H. Jiang,[16] A. Kapoor,[16,l] H. Liao,[16] Z.-A. Liu,[16,m] R. Sharma,[16,n] J. N. Song,[16,m] J. Tao,[16] C. Wang,[16,k] J. Wang,[16] Z. Wang,[16,k] H. Zhang,[16] A. Agapitos,[17] Y. Ban,[17] A. Levin,[17] C. Li,[17] Q. Li,[17] Y. Mao,[17] S. J. Qian,[17] X. Sun,[17] D. Wang,[17] H. Yang,[17] L. Zhang,[17] C. Zhou,[17] Z. You,[18] K. Jaffel,[19] N. Lu,[19] G. Bauer,[20,o] X. Gao,[21,p] Z. Lin,[22] C. Lu,[22] M. Xiao,[22] C. Avila,[23] D. A. Barbosa Trujillo,[23] A. Cabrera,[23] C. Florez,[23] J. Fraga,[23] J. A. Reyes Vega,[23] J. Mejia Guisao,[24] F. Ramirez,[24] M. Rodriguez,[24] J. D. Ruiz Alvarez,[24] D. Giljanovic,[25] N. Godinovic,[25] D. Lelas,[25] A. Sculac,[25] M. Kovac,[26] T. Sculac,[26] P. Bargassa,[27] V. Brigljevic,[27] B. K. Chitroda,[27] D. Ferencek,[27] K. Jakovcic,[27] S. Mishra,[27] A. Starodumov,[27,q] T. Susa,[27] A. Attikis,[28] K. Christoforou,[28] A. Hadjiagapiou,[28] S. Konstantinou,[28] J. Mousa,[28] C. Nicolaou,[28] F. Ptochos,[28] P. A. Razis,[28] H. Rykaczewski,[28] H. Saka,[28] A. Stepennov,[28] M. Finger,[29] M. Finger Jr.,[29] A. Kveton,[29] E. Ayala,[30] E. Carrera Jarrin,[31] S. Elgammal,[32,r] A. Ellithi Kamel,[32,s] M. A. Mahmoud,[33] Y. Mohammed,[33] K. Ehataht,[34] M. Kadastik,[34] T. Lange,[34] S. Nandan,[34] C. Nielsen,[34] J. Pata,[34] M. Raidal,[34] L. Tani,[34] C. Veelken,[34] H. Kirschenmann,[35] K. Osterberg,[35] M. Voutilainen,[35] S. Bharthuar,[36] E. Brücken,[36] F. Garcia,[36] K. T. S. Kallonen,[36] R. Kinnunen,[36] T. Lampén,[36] K. Lassila-Perini,[36] S. Lehti,[36] T. Lindén,[36] L. Martikainen,[36] M. Myllymäki,[36] M. m. Rantanen,[36] H. Siikonen,[36] E. Tuominen,[36] J. Tuominiemi,[36] P. Luukka,[37] H. Petrow,[37] M. Besancon,[38] F. Couderc,[38] M. Dejardin,[38] D. Denegri,[38] J. L. Faure,[38] F. Ferri,[38] S. Ganjour,[38] P. Gras,[38] G. Hamel de Monchenault,[38] V. Lohezic,[38] J. Malcles,[38] J. Rander,[38] A. Rosowsky,[38] M. Ö. Sahin,[38] A. Savoy-Navarro,[38,t] P. Simkina,[38] M. Titov,[38] M. Tornago,[38] F. Beaudette,[39] A. Buchot Perraguin,[39] P. Busson,[39] A. Cappati,[39] C. Charlot,[39] M. Chiusi,[39] F. Damas,[39] O. Davignon,[39] A. De Wit,[39] I. T. Ehle,[39] B. A. Fontana Santos Alves,[39] S. Ghosh,[39] A. Gilbert,[39] R. Granier de Cassagnac,[39] A. Hakimi,[39] B. Harikrishnan,[39] L. Kalipoliti,[39] G. Liu,[39] J. Motta,[39] M. Nguyen,[39] C. Ochando,[39] L. Portales,[39] R. Salerno,[39] J. B. Sauvan,[39] Y. Sirois,[39] A. Tarabini,[39] E. Vernazza,[39] A. Zabi,[39] A. Zghiche,[39] J.-L. Agram,[40,u] J. Andrea,[40] D. Apparu,[40] D. Bloch,[40] J.-M. Brom,[40] E. C. Chabert,[40] C. Collard,[40] S. Falke,[40]

U. Goerlach,[40] C. Grimault,[40] R. Haeberle,[40] A.-C. Le Bihan,[40] M. Meena,[40] G. Saha,[40] M. A. Sessini,[40] P. Van Hove,[40] S. Beauceron,[41] B. Blancon,[41] G. Boudoul,[41] N. Chanon,[41] J. Choi,[41] D. Contardo,[41] P. Depasse,[41] C. Dozen,[41,v] H. El Mamouni,[41] J. Fay,[41] S. Gascon,[41] M. Gouzevitch,[41] C. Greenberg,[41] G. Grenier,[41] B. Ille,[41] I. B. Laktineh,[41] M. Lethuillier,[41] L. Mirabito,[41] S. Perries,[41] A. Purohit,[41] M. Vander Donckt,[41] P. Verdier,[41] J. Xiao,[41] I. Lomidze,[42] T. Toriashvili,[42,w] Z. Tsamalaidze,[42,q] V. Botta,[43] L. Feld,[43] K. Klein,[43] M. Lipinski,[43] D. Meuser,[43] A. Pauls,[43] N. Röwert,[43] M. Teroerde,[43] S. Diekmann,[44] A. Dodonova,[44] N. Eich,[44] D. Eliseev,[44] F. Engelke,[44] J. Erdmann,[44] M. Erdmann,[44] P. Fackeldey,[44] B. Fischer,[44] T. Hebbeker,[44] K. Hoepfner,[44] F. Ivone,[44] A. Jung,[44] M. y. Lee,[44] F. Mausolf,[44] M. Merschmeyer,[44] A. Meyer,[44] S. Mukherjee,[44] D. Noll,[44] F. Nowotny,[44] A. Pozdnyakov,[44] Y. Rath,[44] W. Redjeb,[44] F. Rehm,[44] H. Reithler,[44] U. Sarkar,[44] V. Sarkisovi,[44] A. Schmidt,[44] A. Sharma,[44] J. L. Spah,[44] A. Stein,[44] F. Torres Da Silva De Araujo,[44,x] S. Wiedenbeck,[44] S. Zaleski,[44] C. Dziwok,[45] G. Flügge,[45] W. Haj Ahmad,[45,y] T. Kress,[45] A. Nowack,[45] O. Pooth,[45] A. Stahl,[45] T. Ziemons,[45] A. Zotz,[45] H. Aarup Petersen,[46] M. Aldaya Martin,[46] J. Alimena,[46] S. Amoroso,[46] Y. An,[46] S. Baxter,[46] M. Bayatmakou,[46] H. Becerril Gonzalez,[46] O. Behnke,[46] A. Belvedere,[46] S. Bhattacharya,[46] F. Blekman,[46,z] K. Borras,[46,aa] A. Campbell,[46] A. Cardini,[46] C. Cheng,[46] F. Colombina,[46] S. Consuegra Rodríguez,[46] G. Correia Silva,[46] M. De Silva,[46] G. Eckerlin,[46] D. Eckstein,[46] L. I. Estevez Banos,[46] O. Filatov,[46] E. Gallo,[46,z] A. Geiser,[46] A. Giraldi,[46] V. Guglielmi,[46] M. Guthoff,[46] A. Hinzmann,[46] A. Jafari,[46,bb] L. Jeppe,[46] N. Z. Jomhari,[46] B. Kaech,[46] M. Kasemann,[46] C. Kleinwort,[46] R. Kogler,[46] M. Komm,[46] D. Krücker,[46] W. Lange,[46] D. Leyva Pernia,[46] K. Lipka,[46,cc] W. Lohmann,[46,dd] R. Mankel,[46] I.-A. Melzer-Pellmann,[46] M. Mendizabal Morentin,[46] A. B. Meyer,[46] G. Milella,[46] A. Mussgiller,[46] L. P. Nair,[46] A. Nürnberg,[46] Y. Otarid,[46] J. Park,[46] D. Pérez Adán,[46] E. Ranken,[46] A. Raspereza,[46] B. Ribeiro Lopes,[46] J. Rübenach,[46] A. Saggio,[46] M. Scham,[46,ee,aa] S. Schnake,[46,aa] P. Schütze,[46] C. Schwanenberger,[46,z] D. Selivanova,[46] K. Sharko,[46] M. Shchedrolosiev,[46] R. E. Sosa Ricardo,[46] D. Stafford,[46] F. Vazzoler,[46] A. Ventura Barroso,[46] R. Walsh,[46] Q. Wang,[46] Y. Wen,[46] K. Wichmann,[46] L. Wiens,[46,aa] C. Wissing,[46] Y. Yang,[46] A. Zimermmane Castro Santos,[46] A. Albrecht,[47] S. Albrecht,[47] M. Antonello,[47] S. Bein,[47] L. Benato,[47] S. Bollweg,[47] M. Bonanomi,[47] P. Connor,[47] K. El Morabit,[47] Y. Fischer,[47] E. Garutti,[47] A. Grohsjean,[47] J. Haller,[47] H. R. Jabusch,[47] G. Kasieczka,[47] P. Keicher,[47] R. Klanner,[47] W. Korcari,[47] T. Kramer,[47] V. Kutzner,[47] F. Labe,[47] J. Lange,[47] A. Lobanov,[47] C. Matthies,[47] A. Mehta,[47] L. Moureaux,[47] M. Mrowietz,[47] A. Nigamova,[47] Y. Nissan,[47] A. Paasch,[47] K. J. Pena Rodriguez,[47] T. Quadfasel,[47] B. Raciti,[47] M. Rieger,[47] D. Savoiu,[47] J. Schindler,[47] P. Schleper,[47] M. Schröder,[47] J. Schwandt,[47] M. Sommerhalder,[47] H. Stadie,[47] G. Steinbrück,[47] A. Tews,[47] M. Wolf,[47] S. Brommer,[48] M. Burkart,[48] E. Butz,[48] T. Chwalek,[48] A. Dierlamm,[48] A. Droll,[48] N. Faltermann,[48] M. Giffels,[48] A. Gottmann,[48] F. Hartmann,[48,ff] R. Hofsaess,[48] M. Horzela,[48] U. Husemann,[48] J. Kieseler,[48] M. Klute,[48] R. Koppenhöfer,[48] J. M. Lawhorn,[48] M. Link,[48] A. Lintuluoto,[48] B. Maier,[48] S. Maier,[48] S. Mitra,[48] M. Mormile,[48] Th. Müller,[48] M. Neukum,[48] M. Oh,[48] E. Pfeffer,[48] M. Presilla,[48] G. Quast,[48] K. Rabbertz,[48] B. Regnery,[48] N. Shadskiy,[48] I. Shvetsov,[48] H. J. Simonis,[48] M. Toms,[48] N. Trevisani,[48] R. F. Von Cube,[48] M. Wassmer,[48] S. Wieland,[48] F. Wittig,[48] R. Wolf,[48] X. Zuo,[48] G. Anagnostou,[49] G. Daskalakis,[49] A. Kyriakis,[49] A. Papadopoulos,[49,ff] A. Stakia,[49] P. Kontaxakis,[50] G. Melachroinos,[50] Z. Painesis,[50] A. Panagiotou,[50] I. Papavergou,[50] I. Paraskevas,[50] N. Saoulidou,[50] K. Theofilatos,[50] E. Tziaferi,[50] K. Vellidis,[50] I. Zisopoulos,[50] G. Bakas,[51] T. Chatzistavrou,[51] G. Karapostoli,[51] K. Kousouris,[51] I. Papakrivopoulos,[51] E. Siamarkou,[51] G. Tsipolitis,[51] A. Zacharopoulou,[51] K. Adamidis,[52] I. Bestintzanos,[52] I. Evangelou,[52] C. Foudas,[52] C. Kamtsikis,[52] P. Katsoulis,[52] P. Kokkas,[52] P. G. Kosmoglou Kioseoglou,[52] N. Manthos,[52] I. Papadopoulos,[52] J. Strologas,[52] M. Bartók,[53,gg] C. Hajdu,[53] D. Horvath,[53,hh,ii] K. Márton,[53] A. J. Rádl,[53,jj] F. Sikler,[53] V. Veszpremi,[53] M. Csanád,[54] K. Farkas,[54] M. M. A. Gadallah,[54,kk] Á. Kadlecsik,[54] P. Major,[54] K. Mandal,[54] G. Pásztor,[54] G. I. Veres,[54] P. Raics,[55] B. Ujvari,[55] G. Zilizi,[55] G. Bencze,[56] S. Czellar,[56] J. Molnar,[56] Z. Szillasi,[56] T. Csorgo,[57,ll] F. Nemes,[57,ll] T. Novak,[57] J. Babbar,[58] S. Bansal,[58] S. B. Beri,[58] V. Bhatnagar,[58] G. Chaudhary,[58] S. Chauhan,[58] N. Dhingra,[58,mm] A. Kaur,[58] A. Kaur,[58] H. Kaur,[58] M. Kaur,[58] S. Kumar,[58] K. Sandeep,[58] T. Sheokand,[58] J. B. Singh,[58] A. Singla,[58] A. Ahmed,[59] A. Bhardwaj,[59] A. Chhetri,[59] B. C. Choudhary,[59] A. Kumar,[59] A. Kumar,[59] M. Naimuddin,[59] K. Ranjan,[59] S. Saumya,[59] S. Baradia,[60] S. Barman,[60,nn] S. Bhattacharya,[60] S. Dutta,[60] S. Dutta,[60] S. Sarkar,[60] M. M. Ameen,[61] P. K. Behera,[61] S. C. Behera,[61] S. Chatterjee,[61] P. Jana,[61]

P. Kalbhor,[61] J. R. Komaragiri,[61,oo] D. Kumar,[61,oo] P. R. Pujahari,[61] N. R. Saha,[61] A. Sharma,[61] A. K. Sikdar,[61] S. Verma,[61] S. Dugad,[62] M. Kumar,[62] G. B. Mohanty,[62] P. Suryadevara,[62] A. Bala,[63] S. Banerjee,[63] R. M. Chatterjee,[63] R. K. Dewanjee,[63,pp] M. Guchait,[63] Sh. Jain,[63] A. Jaiswal,[63] S. Karmakar,[63] S. Kumar,[63] G. Majumder,[63] K. Mazumdar,[63] S. Parolia,[63] A. Thachayath,[63] S. Bahinipati,[64,qq] C. Kar,[64] D. Maity,[64,rr] P. Mal,[64] T. Mishra,[64] V. K. Muraleedharan Nair Bindhu,[64,rr] K. Naskar,[64,rr] A. Nayak,[64,rr] P. Sadangi,[64] S. K. Swain,[64] S. Varghese,[64,rr] D. Vats,[64,rr] S. Acharya,[65,ss] A. Alpana,[65] S. Dube,[65] B. Gomber,[65,ss] B. Kansal,[65] A. Laha,[65] B. Sahu,[65,ss] S. Sharma,[65] K. Y. Vaish,[65] H. Bakhshiansohi,[66,tt] E. Khazaie,[66,uu] M. Zeinali,[66,vv] S. Chenarani,[67,ww] S. M. Etesami,[67] M. Khakzad,[67] M. Mohammadi Najafabadi,[67] M. Grunewald,[68] M. Abbrescia,[69a,69b] R. Aly,[69a,69c,xx] A. Colaleo,[69a,69b] D. Creanza,[69a,69c] B. D'Anzi,[69a,69b] N. De Filippis,[69a,69c] M. De Palma,[69a,69b] A. Di Florio,[69a,69c] W. Elmetenawee,[69a,69b,xx] L. Fiore,[69a] G. Iaselli,[69a,69c] M. Louka,[69a,69b] G. Maggi,[69a,69c] M. Maggi,[69a] I. Margjeka,[69a,69b] V. Mastrapasqua,[69a,69b] S. My,[69a,69b] S. Nuzzo,[69a,69b] A. Pellecchia,[69a,69b] A. Pompili,[69a,69b] G. Pugliese,[69a,69c] R. Radogna,[69a] G. Ramirez-Sanchez,[69a,69c] D. Ramos,[69a] A. Ranieri,[69a] L. Silvestris,[69a] F. M. Simone,[69a,69b] Ü. Sözbilir,[69a] A. Stamerra,[69a] R. Venditti,[69a] P. Verwilligen,[69a] A. Zaza,[69a,69b] G. Abbiendi,[70a] C. Battilana,[70a,70b] D. Bonacorsi,[70a,70b] L. Borgonovi,[70a] R. Campanini,[70a,70b] P. Capiluppi,[70a,70b] F. R. Cavallo,[70a] M. Cuffiani,[70a,70b] G. M. Dallavalle,[70a] T. Diotalevi,[70a,70b] F. Fabbri,[70a] A. Fanfani,[70a,70b] D. Fasanella,[70a,70b] P. Giacomelli,[70a] L. Giommi,[70a,70b] C. Grandi,[70a] L. Guiducci,[70a,70b] S. Lo Meo,[70a,yy] L. Lunerti,[70a,70b] S. Marcellini,[70a] G. Masetti,[70a] F. L. Navarria,[70a,70b] A. Perrotta,[70a] F. Primavera,[70a,70b] A. M. Rossi,[70a,70b] T. Rovelli,[70a,70b] G. P. Siroli,[70a,70b] S. Costa,[71a,71b,zz] A. Di Mattia,[71a] R. Potenza,[71a,71b] A. Tricomi,[71a,71b,zz] C. Tuve,[71a,71b] P. Assiouras,[72a] G. Barbagli,[72a] G. Bardelli,[72a,72b] B. Camaiani,[72a,72b] A. Cassese,[72a] R. Ceccarelli,[72a] V. Ciulli,[72a,72b] C. Civinini,[72a] R. D'Alessandro,[72a,72b] E. Focardi,[72a,72b] T. Kello,[72a] G. Latino,[72a,72b] P. Lenzi,[72a,72b] M. Lizzo,[72a] M. Meschini,[72a] S. Paoletti,[72a] A. Papanastassiou,[72a,72b] G. Sguazzoni,[72a] L. Viliani,[72a] L. Benussi,[73] S. Bianco,[73] S. Meola,[73,aaa] D. Piccolo,[73] P. Chatagnon,[74a] F. Ferro,[74a] E. Robutti,[74a] S. Tosi,[74a,74b] A. Benaglia,[75a] G. Boldrini,[75a,75b] F. Brivio,[75a] F. Cetorelli,[75a] F. De Guio,[75a,75b] M. E. Dinardo,[75a,75b] P. Dini,[75a] S. Gennai,[75a] R. Gerosa,[75a,75b] A. Ghezzi,[75a,75b] P. Govoni,[75a,75b] L. Guzzi,[75a] M. T. Lucchini,[75a,75b] M. Malberti,[75a] S. Malvezzi,[75a] A. Massironi,[75a] D. Menasce,[75a] L. Moroni,[75a] M. Paganoni,[75a,75b] D. Pedrini,[75a] B. S. Pinolini,[75a] S. Ragazzi,[75a,75b] T. Tabarelli de Fatis,[75a,75b] D. Zuolo,[75a] S. Buontempo,[76a] A. Cagnotta,[76a,76b] F. Carnevali,[76a,76b] N. Cavallo,[76a,76c] F. Fabozzi,[76a,76c] A. O. M. Iorio,[76a,76b] L. Lista,[76a,76b,bbb] P. Paolucci,[76a,ff] B. Rossi,[76a] C. Sciacca,[76a,76b] R. Ardino,[77a] P. Azzi,[77a] N. Bacchetta,[77a,ccc] D. Bisello,[77a,77b] P. Bortignon,[77a] G. Bortolato,[77a,77b] A. Bragagnolo,[77a,77b] R. Carlin,[77a,77b] T. Dorigo,[77a] F. Gasparini,[77a,77b] U. Gasparini,[77a,77b] E. Lusiani,[77a] M. Margoni,[77a,77b] F. Marini,[77a] A. T. Meneguzzo,[77a,77b] M. Migliorini,[77a,77b] F. Montecassiano,[77a] J. Pazzini,[77a,77b] P. Ronchese,[77a,77b] R. Rossin,[77a,77b] F. Simonetto,[77a,77b] G. Strong,[77a] M. Tosi,[77a,77b] A. Triossi,[77a,77b] S. Ventura,[77a] H. Yarar,[77a,77b] M. Zanetti,[77a,77b] P. Zotto,[77a,77b] A. Zucchetta,[77a,77b] G. Zumerle,[77a,77b] S. Abu Zeid,[78a,ddd] C. Aimè,[78a,78b] A. Braghieri,[78a] S. Calzaferri,[78a] D. Fiorina,[78a] P. Montagna,[78a,78b] V. Re,[78a] C. Riccardi,[78a,78b] P. Salvini,[78a] I. Vai,[78a,78b] P. Vitulo,[78a,78b] S. Ajmal,[79a,79b] G. M. Bilei,[79a] D. Ciangottini,[79a,79b] L. Fanò,[79a,79b] M. Magherini,[79a,79b] G. Mantovani,[79a,79b] V. Mariani,[79a,79b] M. Menichelli,[79a] F. Moscatelli,[79a,eee] A. Rossi,[79a,79b] A. Santocchia,[79a,79b] D. Spiga,[79a] T. Tedeschi,[79a,79b] P. Asenov,[80a,80b] P. Azzurri,[80a] G. Bagliesi,[80a] R. Bhattacharya,[80a] L. Bianchini,[80a,80b] T. Boccali,[80a] E. Bossini,[80a] D. Bruschini,[80a,80c] R. Castaldi,[80a] M. A. Ciocci,[80a,80b] M. Cipriani,[80a,80b] V. D'Amante,[80a,80d] R. Dell'Orso,[80a] S. Donato,[80a] A. Giassi,[80a] F. Ligabue,[80a,80c] D. Matos Figueiredo,[80a] A. Messineo,[80a,80b] M. Musich,[80a,80b] F. Palla,[80a] A. Rizzi,[80a,80b] G. Rolandi,[80a,80c] S. Roy Chowdhury,[80a] T. Sarkar,[80a] A. Scribano,[80a] P. Spagnolo,[80a] R. Tenchini,[80a] G. Tonelli,[80a,80b] N. Turini,[80a,80d] F. Vaselli,[80a,80c] A. Venturi,[80a] P. G. Verdini,[80a] C. Baldenegro Barrera,[81a,81b] P. Barria,[81a] C. Basile,[81a,81b] M. Campana,[81a,81b] F. Cavallari,[81a] L. Cunqueiro Mendez,[81a,81b] D. Del Re,[81a,81b] E. Di Marco,[81a] M. Diemoz,[81a] F. Errico,[81a,81b] E. Longo,[81a,81b] P. Meridiani,[81a] J. Mijuskovic,[81a,81b] G. Organtini,[81a,81b] F. Pandolfi,[81a] R. Paramatti,[81a,81b] C. Quaranta,[81a,81b] S. Rahatlou,[81a,81b] C. Rovelli,[81a] F. Santanastasio,[81a,81b] L. Soffi,[81a] N. Amapane,[82a,82b] R. Arcidiacono,[82a,82c] S. Argiro,[82a,82b] M. Arneodo,[82a,82c] N. Bartosik,[82a] R. Bellan,[82a,82b] A. Bellora,[82a,82b] C. Biino,[82a] C. Borca,[82a,82b] N. Cartiglia,[82a] M. Costa,[82a,82b] R. Covarelli,[82a,82b] N. Demaria,[82a] L. Finco,[82a] M. Grippo,[82a,82b] B. Kiani,[82a,82b] F. Legger,[82a] F. Luongo,[82a,82b] C. Mariotti,[82a] L. Markovic,[82a,82b] S. Maselli,[82a] A. Mecca,[82a,82b]

E. Migliore,[82a,82b] M. Monteno,[82a] R. Mulargia,[82a] M. M. Obertino,[82a,82b] G. Ortona,[82a] L. Pacher,[82a,82b] N. Pastrone,[82a] M. Pelliccioni,[82a] M. Ruspa,[82a,82c] F. Siviero,[82a,82b] V. Sola,[82a,82b] A. Solano,[82a,82b] A. Staiano,[82a] C. Tarricone,[82a,82b] D. Trocino,[82a] G. Umoret,[82a,82b] E. Vlasov,[82a,82b] R. White,[82a] S. Belforte,[83a] V. Candelise,[83a,83b] M. Casarsa,[83a] F. Cossutti,[83a] K. De Leo,[83a] G. Della Ricca,[83a,83b] S. Dogra,[84] J. Hong,[84] C. Huh,[84] B. Kim,[84] D. H. Kim,[84] J. Kim,[84] H. Lee,[84] S. W. Lee,[84] C. S. Moon,[84] Y. D. Oh,[84] M. S. Ryu,[84] S. Sekmen,[84] Y. C. Yang,[84] M. S. Kim,[85] G. Bak,[86] P. Gwak,[86] H. Kim,[86] D. H. Moon,[86] E. Asilar,[87] D. Kim,[87] T. J. Kim,[87] J. A. Merlin,[87] S. Choi,[88] S. Han,[88] B. Hong,[88] K. Lee,[88] K. S. Lee,[88] S. Lee,[88] J. Park,[88] S. K. Park,[88] J. Yoo,[88] J. Goh,[89] S. Yang,[89] H. S. Kim,[90] Y. Kim,[90] S. Lee,[90] J. Almond,[91] J. H. Bhyun,[91] J. Choi,[91] W. Jun,[91] J. Kim,[91] S. Ko,[91] H. Kwon,[91] H. Lee,[91] J. Lee,[91] J. Lee,[91] B. H. Oh,[91] S. B. Oh,[91] H. Seo,[91] U. K. Yang,[91] I. Yoon,[91] W. Jang,[92] D. Y. Kang,[92] Y. Kang,[92] S. Kim,[92] B. Ko,[92] J. S. H. Lee,[92] Y. Lee,[92] I. C. Park,[92] Y. Roh,[92] I. J. Watson,[92] S. Ha,[93] H. D. Yoo,[93] M. Choi,[94] M. R. Kim,[94] H. Lee,[94] Y. Lee,[94] I. Yu,[94] T. Beyrouthy,[95] K. Dreimanis,[96] A. Gaile,[96] G. Pikurs,[96] A. Potrebko,[96] M. Seidel,[96] N. R. Strautnieks,[97] M. Ambrozas,[98] A. Juodagalvis,[98] A. Rinkevicius,[98] G. Tamulaitis,[98] N. Bin Norjoharuddeen,[99] I. Yusuff,[99,fff] Z. Zolkapli,[99] J. F. Benitez,[100] A. Castaneda Hernandez,[100] H. A. Encinas Acosta,[100] L. G. Gallegos Maríñez,[100] M. León Coello,[100] J. A. Murillo Quijada,[100] A. Sehrawat,[100] L. Valencia Palomo,[100] G. Ayala,[101] H. Castilla-Valdez,[101] H. Crotte Ledesma,[101] E. De La Cruz-Burelo,[101] I. Heredia-De La Cruz,[101,ggg] R. Lopez-Fernandez,[101] C. A. Mondragon Herrera,[101] A. Sánchez Hernández,[101] C. Oropeza Barrera,[102] M. Ramírez García,[102] I. Bautista,[103] I. Pedraza,[103] H. A. Salazar Ibarguen,[103] C. Uribe Estrada,[103] I. Bubanja,[104] N. Raicevic,[104] P. H. Butler,[105] A. Ahmad,[106] M. I. Asghar,[106] A. Awais,[106] M. I. M. Awan,[106] H. R. Hoorani,[106] W. A. Khan,[106] V. Avati,[107] L. Grzanka,[107] M. Malawski,[107] H. Bialkowska,[108] M. Bluj,[108] B. Boimska,[108] M. Górski,[108] M. Kazana,[108] M. Szleper,[108] P. Zalewski,[108] K. Bunkowski,[109] K. Doroba,[109] A. Kalinowski,[109] M. Konecki,[109] J. Krolikowski,[109] A. Muhammad,[109] K. Pozniak,[110] W. Zabolotny,[110] M. Araujo,[111] D. Bastos,[111] C. Beirão Da Cruz E Silva,[111] A. Boletti,[111] M. Bozzo,[111] T. Camporesi,[111] G. Da Molin,[111] P. Faccioli,[111] M. Gallinaro,[111] J. Hollar,[111] N. Leonardo,[111] T. Niknejad,[111] A. Petrilli,[111] M. Pisano,[111] J. Seixas,[111] J. Varela,[111] J. W. Wulff,[111] P. Adzic,[112] P. Milenovic,[112] M. Dordevic,[113] J. Milosevic,[113] V. Rekovic,[113] M. Aguilar-Benitez,[114] J. Alcaraz Maestre,[114] Cristina F. Bedoya,[114] Oliver M. Carretero,[114] M. Cepeda,[114] M. Cerrada,[114] N. Colino,[114] B. De La Cruz,[114] A. Delgado Peris,[114] A. Escalante Del Valle,[114] D. Fernández Del Val,[114] J. P. Fernández Ramos,[114] J. Flix,[114] M. C. Fouz,[114] O. Gonzalez Lopez,[114] S. Goy Lopez,[114] J. M. Hernandez,[114] M. I. Josa,[114] D. Moran,[114] C. M. Morcillo Perez,[114] Á. Navarro Tobar,[114] C. Perez Dengra,[114] A. Pérez-Calero Yzquierdo,[114] J. Puerta Pelayo,[114] I. Redondo,[114] D. D. Redondo Ferrero,[114] L. Romero,[114] S. Sánchez Navas,[114] L. Urda Gómez,[114] J. Vazquez Escobar,[114] C. Willmott,[114] J. F. de Trocóniz,[115] B. Alvarez Gonzalez,[116] J. Cuevas,[116] J. Fernandez Menendez,[116] S. Folgueras,[116] I. Gonzalez Caballero,[116] J. R. González Fernández,[116] P. Leguina,[116] E. Palencia Cortezon,[116] C. Ramón Álvarez,[116] V. Rodríguez Bouza,[116] A. Soto Rodríguez,[116] A. Trapote,[116] C. Vico Villalba,[116] P. Vischia,[116] S. Bhowmik,[117] S. Blanco Fernández,[117] J. A. Brochero Cifuentes,[117] I. J. Cabrillo,[117] A. Calderon,[117] J. Duarte Campderros,[117] M. Fernandez,[117] G. Gomez,[117] C. Lasaosa García,[117] C. Martinez Rivero,[117] P. Martinez Ruiz del Arbol,[117] F. Matorras,[117] P. Matorras Cuevas,[117] E. Navarrete Ramos,[117] J. Piedra Gomez,[117] L. Scodellaro,[117] I. Vila,[117] J. M. Vizan Garcia,[117] M. K. Jayananda,[118] B. Kailasapathy,[118,hhh] D. U. J. Sonnadara,[118] D. D. C. Wickramarathna,[118] W. G. D. Dharmaratna,[119,iii] K. Liyanage,[119] N. Perera,[119] N. Wickramage,[119] D. Abbaneo,[120] C. Amendola,[120] E. Auffray,[120] G. Auzinger,[120] J. Baechler,[120] D. Barney,[120] A. Bermúdez Martínez,[120] M. Bianco,[120] B. Bilin,[120] A. A. Bin Anuar,[120] A. Bocci,[120] C. Botta,[120] E. Brondolin,[120] C. Caillol,[120] G. Cerminara,[120] N. Chernyavskaya,[120] D. d'Enterria,[120] A. Dabrowski,[120] A. David,[120] A. De Roeck,[120] M. M. Defranchis,[120] M. Deile,[120] M. Dobson,[120] L. Forthomme,[120] G. Franzoni,[120] W. Funk,[120] S. Giani,[120] D. Gigi,[120] K. Gill,[120] F. Glege,[120] L. Gouskos,[120] M. Haranko,[120] J. Hegeman,[120] B. Huber,[120] V. Innocente,[120] T. James,[120] P. Janot,[120] O. Kaluzinska,[120] S. Laurila,[120] P. Lecoq,[120] E. Leutgeb,[120] C. Lourenço,[120] L. Malgeri,[120] M. Mannelli,[120] A. C. Marini,[120] M. Matthewman,[120] F. Meijers,[120] S. Mersi,[120] E. Meschi,[120] V. Milosevic,[120] F. Monti,[120] F. Moortgat,[120] M. Mulders,[120] I. Neutelings,[120] S. Orfanelli,[120] F. Pantaleo,[120] G. Petrucciani,[120] A. Pfeiffer,[120] M. Pierini,[120] D. Piparo,[120] H. Qu,[120] D. Rabady,[120] M. Rovere,[120] H. Sakulin,[120] S. Scarfi,[120] C. Schwick,[120] M. Selvaggi,[120] A. Sharma,[120]

K. Shchelina,[120] P. Silva,[120] P. Sphicas,[120,jjj] A. G. Stahl Leiton,[120] A. Steen,[120] S. Summers,[120] D. Treille,[120] P. Tropea,[120] A. Tsirou,[120] D. Walter,[120] J. Wanczyk,[120,kkk] J. Wang,[120] S. Wuchterl,[120] P. Zehetner,[120] P. Zejdl,[120] W. D. Zeuner,[120] T. Bevilacqua,[121,lll] L. Caminada,[121,lll] A. Ebrahimi,[121] W. Erdmann,[121] R. Horisberger,[121] Q. Ingram,[121] H. C. Kaestli,[121] D. Kotlinski,[121] C. Lange,[121] M. Missiroli,[121,lll] L. Noehte,[121,lll] T. Rohe,[121] T. K. Aarrestad,[122] K. Androsov,[122,kkk] M. Backhaus,[122] A. Calandri,[122] C. Cazzaniga,[122] K. Datta,[122] A. De Cosa,[122] G. Dissertori,[122] M. Dittmar,[122] M. Donegà,[122] F. Eble,[122] M. Galli,[122] K. Gedia,[122] F. Glessgen,[122] C. Grab,[122] N. Härringer,[122] T. G. Harte,[122] D. Hits,[122] W. Lustermann,[122] A.-M. Lyon,[122] R. A. Manzoni,[122] M. Marchegiani,[122] L. Marchese,[122] C. Martin Perez,[122] A. Mascellani,[122,kkk] F. Nessi-Tedaldi,[122] F. Pauss,[122] V. Perovic,[122] S. Pigazzini,[122] C. Reissel,[122] T. Reitenspiess,[122] B. Ristic,[122] F. Riti,[122] R. Seidita,[122] J. Steggemann,[122,kkk] D. Valsecchi,[122] R. Wallny,[122] C. Amsler,[123,mmm] P. Bärtschi,[123] M. F. Canelli,[123] K. Cormier,[123] J. K. Heikkilä,[123] M. Huwiler,[123] W. Jin,[123] A. Jofrehei,[123] B. Kilminster,[123] S. Leontsinis,[123] S. P. Liechti,[123] A. Macchiolo,[123] P. Meiring,[123] U. Molinatti,[123] A. Reimers,[123] P. Robmann,[123] S. Sanchez Cruz,[123] M. Senger,[123] F. Stäger,[123] Y. Takahashi,[123] R. Tramontano,[123] C. Adloff,[124,nnn] D. Bhowmik,[124] C. M. Kuo,[124] W. Lin,[124] P. K. Rout,[124] P. C. Tiwari,[124,oo] S. S. Yu,[124] L. Ceard,[125] Y. Chao,[125] K. F. Chen,[125] P. s. Chen,[125] Z. g. Chen,[125] A. De Iorio,[125] W.-S. Hou,[125] T. h. Hsu,[125] Y. w. Kao,[125] R. Khurana,[125] G. Kole,[125] Y. y. Li,[125] R.-S. Lu,[125] E. Paganis,[125] X. f. Su,[125] J. Thomas-Wilsker,[125] L. s. Tsai,[125] H. y. Wu,[125] E. Yazgan,[125] C. Asawatangtrakuldee,[126] N. Srimanobhas,[126] V. Wachirapusitanand,[126] D. Agyel,[127] F. Boran,[127] Z. S. Demiroglu,[127] F. Dolek,[127] I. Dumanoglu,[127,ooo] E. Eskut,[127] Y. Guler,[127,ppp] E. Gurpinar Guler,[127,ppp] C. Isik,[127] O. Kara,[127] A. Kayis Topaksu,[127] U. Kiminsu,[127] G. Onengut,[127] K. Ozdemir,[127,qqq] A. Polatoz,[127] B. Tali,[127,rrr] U. G. Tok,[127] S. Turkcapar,[127] E. Uslan,[127] I. S. Zorbakir,[127] M. Yalvac,[128,sss] B. Akgun,[129] I. O. Atakisi,[129] E. Gülmez,[129] M. Kaya,[129,ttt] O. Kaya,[129,uuu] S. Tekten,[129,vvv] A. Cakir,[130] K. Cankocak,[130,ooo,www] G. G. Dincer,[130] Y. Komurcu,[130] S. Sen,[130,xxx] O. Aydilek,[131,y] S. Cerci,[131,rrr] V. Epshteyn,[131] B. Hacisahinoglu,[131] I. Hos,[131,yyy] B. Kaynak,[131] S. Ozkorucuklu,[131] O. Potok,[131] H. Sert,[131] C. Simsek,[131] C. Zorbilmez,[131] B. Isildak,[132,zzz] D. Sunar Cerci,[132,rrr] A. Boyaryntsev,[133] B. Grynyov,[133] L. Levchuk,[134] D. Anthony,[135] J. J. Brooke,[135] A. Bundock,[135] F. Bury,[135] E. Clement,[135] D. Cussans,[135] H. Flacher,[135] M. Glowacki,[135] J. Goldstein,[135] H. F. Heath,[135] M.-L. Holmberg,[135] L. Kreczko,[135] S. Paramesvaran,[135] L. Robertshaw,[135] S. Seif El Nasr-Storey,[135] V. J. Smith,[135] N. Stylianou,[135,aaaa] K. Walkingshaw Pass,[135] A. H. Ball,[136] K. W. Bell,[136] A. Belyaev,[136,bbbb] C. Brew,[136] R. M. Brown,[136] D. J. A. Cockerill,[136] C. Cooke,[136] K. V. Ellis,[136] K. Harder,[136] S. Harper,[136] J. Linacre,[136] K. Manolopoulos,[136] D. M. Newbold,[136] E. Olaiya,[136] D. Petyt,[136] T. Reis,[136] A. R. Sahasransu,[136] G. Salvi,[136] T. Schuh,[136] C. H. Shepherd-Themistocleous,[136] I. R. Tomalin,[136] T. Williams,[136] R. Bainbridge,[137] P. Bloch,[137] C. E. Brown,[137] O. Buchmuller,[137] V. Cacchio,[137] C. A. Carrillo Montoya,[137] G. S. Chahal,[137,cccc] D. Colling,[137] J. S. Dancu,[137] I. Das,[137] P. Dauncey,[137] G. Davies,[137] J. Davies,[137] M. Della Negra,[137] S. Fayer,[137] G. Fedi,[137] G. Hall,[137] M. H. Hassanshahi,[137] A. Howard,[137] G. Iles,[137] M. Knight,[137] J. Langford,[137] J. León Holgado,[137] L. Lyons,[137] A.-M. Magnan,[137] S. Malik,[137] M. Mieskolainen,[137] J. Nash,[137,dddd] M. Pesaresi,[137] B. C. Radburn-Smith,[137] A. Richards,[137] A. Rose,[137] K. Savva,[137] C. Seez,[137] R. Shukla,[137] A. Tapper,[137] K. Uchida,[137] G. P. Uttley,[137] L. H. Vage,[137] T. Virdee,[137,ff] M. Vojinovic,[137] N. Wardle,[137] D. Winterbottom,[137] K. Coldham,[138] J. E. Cole,[138] A. Khan,[138] P. Kyberd,[138] I. D. Reid,[138] S. Abdullin,[139] A. Brinkerhoff,[139] B. Caraway,[139] E. Collins,[139] J. Dittmann,[139] K. Hatakeyama,[139] J. Hiltbrand,[139] B. McMaster,[139] M. Saunders,[139] S. Sawant,[139] C. Sutantawibul,[139] J. Wilson,[139] R. Bartek,[140] A. Dominguez,[140] C. Huerta Escamilla,[140] A. E. Simsek,[140] R. Uniyal,[140] A. M. Vargas Hernandez,[140] B. Bam,[141] R. Chudasama,[141] S. I. Cooper,[141] S. V. Gleyzer,[141] C. U. Perez,[141] P. Rumerio,[141,eeee] E. Usai,[141] R. Yi,[141] A. Akpinar,[142] D. Arcaro,[142] C. Cosby,[142] Z. Demiragli,[142] C. Erice,[142] C. Fangmeier,[142] C. Fernandez Madrazo,[142] E. Fontanesi,[142] D. Gastler,[142] F. Golf,[142] S. Jeon,[142] I. Reed,[142] J. Rohlf,[142] K. Salyer,[142] D. Sperka,[142] D. Spitzbart,[142] I. Suarez,[142] A. Tsatsos,[142] S. Yuan,[142] A. G. Zecchinelli,[142] G. Benelli,[143] X. Coubez,[143,aa] D. Cutts,[143] M. Hadley,[143] U. Heintz,[143] J. M. Hogan,[143,ffff] T. Kwon,[143] G. Landsberg,[143] K. T. Lau,[143] D. Li,[143] J. Luo,[143] S. Mondal,[143] M. Narain,[143,a] N. Pervan,[143] S. Sagir,[143,gggg] F. Simpson,[143] M. Stamenkovic,[143] X. Yan,[143] W. Zhang,[143] S. Abbott,[144] J. Bonilla,[144] C. Brainerd,[144] R. Breedon,[144] H. Cai,[144] M. Calderon De La Barca Sanchez,[144] M. Chertok,[144] M. Citron,[144] J. Conway,[144] P. T. Cox,[144]

R. Erbacher,[144] F. Jensen,[144] O. Kukral,[144] G. Mocellin,[144] M. Mulhearn,[144] D. Pellett,[144] W. Wei,[144] Y. Yao,[144] F. Zhang,[144] M. Bachtis,[145] R. Cousins,[145] A. Datta,[145] G. Flores Avila,[145] J. Hauser,[145] M. Ignatenko,[145] M. A. Iqbal,[145] T. Lam,[145] E. Manca,[145] A. Nunez Del Prado,[145] D. Saltzberg,[145] V. Valuev,[145] R. Clare,[146] J. W. Gary,[146] M. Gordon,[146] G. Hanson,[146] W. Si,[146] S. Wimpenny,[146,a] J. G. Branson,[147] S. Cittolin,[147] S. Cooperstein,[147] D. Diaz,[147] J. Duarte,[147] L. Giannini,[147] J. Guiang,[147] R. Kansal,[147] V. Krutelyov,[147] R. Lee,[147] J. Letts,[147] M. Masciovecchio,[147] F. Mokhtar,[147] S. Mukherjee,[147] M. Pieri,[147] M. Quinnan,[147] B. V. Sathia Narayanan,[147] V. Sharma,[147] M. Tadel,[147] E. Vourliotis,[147] F. Würthwein,[147] Y. Xiang,[147] A. Yagil,[147] A. Barzdukas,[148] L. Brennan,[148] C. Campagnari,[148] J. Incandela,[148] J. Kim,[148] A. J. Li,[148] P. Masterson,[148] H. Mei,[148] J. Richman,[148] U. Sarica,[148] R. Schmitz,[148] F. Setti,[148] J. Sheplock,[148] D. Stuart,[148] T. Á. Vámi,[148] S. Wang,[148] A. Bornheim,[149] O. Cerri,[149] A. Latorre,[149] J. Mao,[149] H. B. Newman,[149] G. Reales Gutiérrez,[149] M. Spiropulu,[149] J. R. Vlimant,[149] C. Wang,[149] S. Xie,[149] R. Y. Zhu,[149] J. Alison,[150] S. An,[150] M. B. Andrews,[150] P. Bryant,[150] M. Cremonesi,[150] V. Dutta,[150] T. Ferguson,[150] A. Harilal,[150] C. Liu,[150] T. Mudholkar,[150] S. Murthy,[150] P. Palit,[150] M. Paulini,[150] A. Roberts,[150] A. Sanchez,[150] W. Terrill,[150] J. P. Cumalat,[151] W. T. Ford,[151] A. Hart,[151] A. Hassani,[151] G. Karathanasis,[151] N. Manganelli,[151] A. Perloff,[151] C. Savard,[151] N. Schonbeck,[151] K. Stenson,[151] K. A. Ulmer,[151] S. R. Wagner,[151] N. Zipper,[151] J. Alexander,[152] S. Bright-Thonney,[152] X. Chen,[152] D. J. Cranshaw,[152] J. Fan,[152] X. Fan,[152] S. Hogan,[152] P. Kotamnives,[152] J. Monroy,[152] M. Oshiro,[152] J. R. Patterson,[152] J. Reichert,[152] M. Reid,[152] A. Ryd,[152] J. Thom,[152] P. Wittich,[152] R. Zou,[152] M. Albrow,[153] M. Alyari,[153] O. Amram,[153] G. Apollinari,[153] A. Apresyan,[153] L. A. T. Bauerdick,[153] D. Berry,[153] J. Berryhill,[153] P. C. Bhat,[153] K. Burkett,[153] J. N. Butler,[153] A. Canepa,[153] G. B. Cerati,[153] H. W. K. Cheung,[153] F. Chlebana,[153] G. Cummings,[153] J. Dickinson,[153] I. Dutta,[153] V. D. Elvira,[153] Y. Feng,[153] J. Freeman,[153] A. Gandrakota,[153] Z. Gecse,[153] L. Gray,[153] D. Green,[153] A. Grummer,[153] S. Grünendahl,[153] D. Guerrero,[153] O. Gutsche,[153] R. M. Harris,[153] R. Heller,[153] T. C. Herwig,[153] J. Hirschauer,[153] L. Horyn,[153] B. Jayatilaka,[153] S. Jindariani,[153] M. Johnson,[153] U. Joshi,[153] T. Klijnsma,[153] B. Klima,[153] K. H. M. Kwok,[153] S. Lammel,[153] D. Lincoln,[153] R. Lipton,[153] T. Liu,[153] C. Madrid,[153] K. Maeshima,[153] C. Mantilla,[153] D. Mason,[153] P. McBride,[153] P. Merkel,[153] S. Mrenna,[153] S. Nahn,[153] J. Ngadiuba,[153] D. Noonan,[153] V. Papadimitriou,[153] N. Pastika,[153] K. Pedro,[153] C. Pena,[153,hhhh] F. Ravera,[153] A. Reinsvold Hall,[153,iiii] L. Ristori,[153] E. Sexton-Kennedy,[153] N. Smith,[153] A. Soha,[153] L. Spiegel,[153] S. Stoynev,[153] J. Strait,[153] L. Taylor,[153] S. Tkaczyk,[153] N. V. Tran,[153] L. Uplegger,[153] E. W. Vaandering,[153] A. Whitbeck,[153] I. Zoi,[153] C. Aruta,[154] P. Avery,[154] D. Bourilkov,[154] L. Cadamuro,[154] P. Chang,[154] V. Cherepanov,[154] R. D. Field,[154] E. Koenig,[154] M. Kolosova,[154] J. Konigsberg,[154] A. Korytov,[154] K. Matchev,[154] N. Menendez,[154] G. Mitselmakher,[154] K. Mohrman,[154] A. Muthirakalayil Madhu,[154] N. Rawal,[154] D. Rosenzweig,[154] S. Rosenzweig,[154] J. Wang,[154] T. Adams,[155] A. Al Kadhim,[155] A. Askew,[155] S. Bower,[155] R. Habibullah,[155] V. Hagopian,[155] R. Hashmi,[155] R. S. Kim,[155] S. Kim,[155] T. Kolberg,[155] G. Martinez,[155] H. Prosper,[155] P. R. Prova,[155] M. Wulansatiti,[155] R. Yohay,[155] J. Zhang,[155] B. Alsufyani,[156] M. M. Baarmand,[156] S. Butalla,[156] S. Das,[156] T. Elkafrawy,[156,ddd] M. Hohlmann,[156] R. Kumar Verma,[156] M. Rahmani,[156] E. Yanes,[156] M. R. Adams,[157] A. Baty,[157] C. Bennett,[157] R. Cavanaugh,[157] R. Escobar Franco,[157] O. Evdokimov,[157] C. E. Gerber,[157] M. Hawksworth,[157] A. Hingrajiya,[157] D. J. Hofman,[157] J. h. Lee,[157] D. S. Lemos,[157] A. H. Merrit,[157] C. Mills,[157] S. Nanda,[157] G. Oh,[157] B. Ozek,[157] D. Pilipovic,[157] R. Pradhan,[157] E. Prifti,[157] T. Roy,[157] S. Rudrabhatla,[157] M. B. Tonjes,[157] N. Varelas,[157] Z. Ye,[157] J. Yoo,[157] M. Alhusseini,[158] D. Blend,[158] K. Dilsiz,[158,jjjj] L. Emediato,[158] G. Karaman,[158] O. K. Köseyan,[158] J.-P. Merlo,[158] A. Mestvirishvili,[158,kkkk] J. Nachtman,[158] O. Neogi,[158] H. Ogul,[158,llll] Y. Onel,[158] A. Penzo,[158] C. Snyder,[158] E. Tiras,[158,mmmm] B. Blumenfeld,[159] L. Corcodilos,[159] J. Davis,[159] A. V. Gritsan,[159] L. Kang,[159] S. Kyriacou,[159] P. Maksimovic,[159] M. Roguljic,[159] J. Roskes,[159] S. Sekhar,[159] M. Swartz,[159] A. Abreu,[160] L. F. Alcerro Alcerro,[160] J. Anguiano,[160] P. Baringer,[160] A. Bean,[160] Z. Flowers,[160] D. Grove,[160] J. King,[160] G. Krintiras,[160] M. Lazarovits,[160] C. Le Mahieu,[160] J. Marquez,[160] N. Minafra,[160] M. Murray,[160] M. Nickel,[160] M. Pitt,[160] S. Popescu,[160,nnnn] C. Rogan,[160] C. Royon,[160] R. Salvatico,[160] S. Sanders,[160] C. Smith,[160] Q. Wang,[160] G. Wilson,[160] B. Allmond,[161] A. Ivanov,[161] K. Kaadze,[161] A. Kalogeropoulos,[161] D. Kim,[161] Y. Maravin,[161] J. Natoli,[161] D. Roy,[161] G. Sorrentino,[161] F. Rebassoo,[162] D. Wright,[162] A. Baden,[163] A. Belloni,[163] Y. M. Chen,[163] S. C. Eno,[163] N. J. Hadley,[163] S. Jabeen,[163] R. G. Kellogg,[163] T. Koeth,[163] Y. Lai,[163] S. Lascio,[163] A. C. Mignerey,[163]

S. Nabili,[163] C. Palmer,[163] C. Papageorgakis,[163] M. M. Paranjpe,[163] L. Wang,[163] J. Bendavid,[164] I. A. Cali,[164] M. D'Alfonso,[164] J. Eysermans,[164] C. Freer,[164] G. Gomez-Ceballos,[164] M. Goncharov,[164] G. Grosso,[164] P. Harris,[164] D. Hoang,[164] D. Kovalskyi,[164] J. Krupa,[164] L. Lavezzo,[164] Y.-J. Lee,[164] K. Long,[164] A. Novak,[164] C. Paus,[164] D. Rankin,[164] C. Roland,[164] G. Roland,[164] S. Rothman,[164] G. S. F. Stephans,[164] Z. Wang,[164] B. Wyslouch,[164] T. J. Yang,[164] B. Crossman,[165] B. M. Joshi,[165] C. Kapsiak,[165] M. Krohn,[165] D. Mahon,[165] J. Mans,[165] B. Marzocchi,[165] S. Pandey,[165] M. Revering,[165] R. Rusack,[165] R. Saradhy,[165] N. Schroeder,[165] N. Strobbe,[165] M. A. Wadud,[165] L. M. Cremaldi,[166] K. Bloom,[167] D. R. Claes,[167] G. Haza,[167] J. Hossain,[167] C. Joo,[167] I. Kravchenko,[167] J. E. Siado,[167] W. Tabb,[167] A. Vagnerini,[167] A. Wightman,[167] F. Yan,[167] D. Yu,[167] H. Bandyopadhyay,[168] L. Hay,[168] I. Iashvili,[168] A. Kharchilava,[168] M. Morris,[168] D. Nguyen,[168] S. Rappoccio,[168] H. Rejeb Sfar,[168] A. Williams,[168] G. Alverson,[169] E. Barberis,[169] J. Dervan,[169] Y. Haddad,[169] Y. Han,[169] A. Krishna,[169] J. Li,[169] M. Lu,[169] G. Madigan,[169] R. Mccarthy,[169] D. M. Morse,[169] V. Nguyen,[169] T. Orimoto,[169] A. Parker,[169] L. Skinnari,[169] B. Wang,[169] D. Wood,[169] S. Bhattacharya,[170] J. Bueghly,[170] Z. Chen,[170] S. Dittmer,[170] K. A. Hahn,[170] Y. Liu,[170] Y. Miao,[170] D. G. Monk,[170] M. H. Schmitt,[170] A. Taliercio,[170] M. Velasco,[170] G. Agarwal,[171] R. Band,[171] R. Bucci,[171] S. Castells,[171] A. Das,[171] R. Goldouzian,[171] M. Hildreth,[171] K. W. Ho,[171] K. Hurtado Anampa,[171] T. Ivanov,[171] C. Jessop,[171] K. Lannon,[171] J. Lawrence,[171] N. Loukas,[171] L. Lutton,[171] J. Mariano,[171] N. Marinelli,[171] I. Mcalister,[171] T. McCauley,[171] C. Mcgrady,[171] C. Moore,[171] Y. Musienko,[171,q] H. Nelson,[171] M. Osherson,[171] A. Piccinelli,[171] R. Ruchti,[171] A. Townsend,[171] Y. Wan,[171] M. Wayne,[171] H. Yockey,[171] M. Zarucki,[171] L. Zygala,[171] A. Basnet,[172] B. Bylsma,[172] M. Carrigan,[172] L. S. Durkin,[172] C. Hill,[172] M. Joyce,[172] M. Nunez Ornelas,[172] K. Wei,[172] B. L. Winer,[172] B. R. Yates,[172] F. M. Addesa,[173] H. Bouchamaoui,[173] P. Das,[173] G. Dezoort,[173] P. Elmer,[173] A. Frankenthal,[173] B. Greenberg,[173] N. Haubrich,[173] G. Kopp,[173] S. Kwan,[173] D. Lange,[173] A. Loeliger,[173] D. Marlow,[173] I. Ojalvo,[173] J. Olsen,[173] A. Shevelev,[173] D. Stickland,[173] C. Tully,[173] S. Malik,[174] A. S. Bakshi,[175] V. E. Barnes,[175] S. Chandra,[175] R. Chawla,[175] A. Gu,[175] L. Gutay,[175] M. Jones,[175] A. W. Jung,[175] D. Kondratyev,[175] A. M. Koshy,[175] M. Liu,[175] G. Negro,[175] N. Neumeister,[175] G. Paspalaki,[175] S. Piperov,[175] V. Scheurer,[175] J. F. Schulte,[175] M. Stojanovic,[175] J. Thieman,[175] A. K. Virdi,[175] F. Wang,[175] W. Xie,[175] J. Dolen,[176] N. Parashar,[176] A. Pathak,[176] D. Acosta,[177] T. Carnahan,[177] K. M. Ecklund,[177] P. J. Fernández Manteca,[177] S. Freed,[177] P. Gardner,[177] F. J. M. Geurts,[177] W. Li,[177] O. Miguel Colin,[177] B. P. Padley,[177] R. Redjimi,[177] J. Rotter,[177] E. Yigitbasi,[177] Y. Zhang,[177] A. Bodek,[178] P. de Barbaro,[178] R. Demina,[178] J. L. Dulemba,[178] A. Garcia-Bellido,[178] O. Hindrichs,[178] A. Khukhunaishvili,[178] N. Parmar,[178] P. Parygin,[178,q] E. Popova,[178,q] R. Taus,[178] K. Goulianos,[179] B. Chiarito,[180] J. P. Chou,[180] S. V. Clark,[180] D. Gadkari,[180] Y. Gershtein,[180] E. Halkiadakis,[180] M. Heindl,[180] C. Houghton,[180] D. Jaroslawski,[180] O. Karacheban,[180,dd] I. Laflotte,[180] A. Lath,[180] R. Montalvo,[180] K. Nash,[180] H. Routray,[180] P. Saha,[180] S. Salur,[180] S. Schnetzer,[180] S. Somalwar,[180] R. Stone,[180] S. A. Thayil,[180] S. Thomas,[180] J. Vora,[180] H. Wang,[180] H. Acharya,[181] D. Ally,[181] A. G. Delannoy,[181] S. Fiorendi,[181] S. Higginbotham,[181] T. Holmes,[181] A. R. Kanuganti,[181] N. Karunarathna,[181] L. Lee,[181] E. Nibigira,[181] S. Spanier,[181] D. Aebi,[182] M. Ahmad,[182] O. Bouhali,[182,oooo] R. Eusebi,[182] J. Gilmore,[182] T. Huang,[182] T. Kamon,[182,pppp] H. Kim,[182] S. Luo,[182] R. Mueller,[182] D. Overton,[182] D. Rathjens,[182] A. Safonov,[182] N. Akchurin,[183] J. Damgov,[183] V. Hegde,[183] A. Hussain,[183] Y. Kazhykarim,[183] K. Lamichhane,[183] S. W. Lee,[183] A. Mankel,[183] T. Peltola,[183] I. Volobouev,[183] E. Appelt,[184] Y. Chen,[184] S. Greene,[184] A. Gurrola,[184] W. Johns,[184] R. Kunnawalkam Elayavalli,[184] A. Melo,[184] F. Romeo,[184] P. Sheldon,[184] S. Tuo,[184] J. Velkovska,[184] J. Viinikainen,[184] B. Cardwell,[185] B. Cox,[185] J. Hakala,[185] R. Hirosky,[185] A. Ledovskoy,[185] C. Neu,[185] C. E. Perez Lara,[185] P. E. Karchin,[186] A. Aravind,[187] S. Banerjee,[187] K. Black,[187] T. Bose,[187] S. Dasu,[187] I. De Bruyn,[187] P. Everaerts,[187] C. Galloni,[187] H. He,[187] M. Herndon,[187] A. Herve,[187] C. K. Koraka,[187] A. Lanaro,[187] R. Loveless,[187] J. Madhusudanan Sreekala,[187] A. Mallampalli,[187] A. Mohammadi,[187] S. Mondal,[187] G. Parida,[187] L. Pétré,[187] D. Pinna,[187] A. Savin,[187] V. Shang,[187] V. Sharma,[187] W. H. Smith,[187] D. Teague,[187] H. F. Tsoi,[187] W. Vetens,[187] A. Warden,[187] S. Afanasiev,[188] V. Andreev,[188] Yu. Andreev,[188] T. Aushev,[188] M. Azarkin,[188] I. Azhgirey,[188] A. Babaev,[188] A. Belyaev,[188] V. Blinov,[188,q] E. Boos,[188] V. Borshch,[188] D. Budkouski,[188] V. Bunichev,[188] M. Chadeeva,[188,q] V. Chekhovsky,[188] R. Chistov,[188,q] A. Dermenev,[188] T. Dimova,[188,q] D. Druzhkin,[188,qqqq] M. Dubinin,[188,hhhh] L. Dudko,[188] A. Ershov,[188] G. Gavrilov,[188] V. Gavrilov,[188] S. Gninenko,[188] V. Golovtcov,[188] N. Golubev,[188] I. Golutvin,[188]

I. Gorbunov,[188] A. Gribushin,[188] Y. Ivanov,[188] V. Kachanov,[188] V. Karjavine,[188] A. Karneyeu,[188] V. Kim,[188,q] M. Kirakosyan,[188] D. Kirpichnikov,[188] M. Kirsanov,[188] V. Klyukhin,[188] O. Kodolova,[188,rrrr] D. Konstantinov,[188] V. Korenkov,[188] A. Kozyrev,[188,q] N. Krasnikov,[188] A. Lanev,[188] P. Levchenko,[188,ssss] N. Lychkovskaya,[188] V. Makarenko,[188] A. Malakhov,[188] V. Matveev,[188,q] V. Murzin,[188] A. Nikitenko,[188,tttt,rrrr] S. Obraztsov,[188] V. Oreshkin,[188] V. Palichik,[188] V. Perelygin,[188] S. Petrushanko,[188] S. Polikarpov,[188,q] V. Popov,[188] O. Radchenko,[188,q] R. Ryutin,[188] M. Savina,[188] V. Savrin,[188] V. Shalaev,[188] S. Shmatov,[188] S. Shulha,[188] Y. Skovpen,[188,q] S. Slabospitskii,[188] V. Smirnov,[188] A. Snigirev,[188] D. Sosnov,[188] V. Sulimov,[188] E. Tcherniaev,[188] A. Terkulov,[188] O. Teryaev,[188] I. Tlisova,[188] A. Toropin,[188] L. Uvarov,[188] A. Uzunian,[188] A. Vorobyev,[188,a] N. Voytishin,[188] B. S. Yuldashev,[188,uuuu] A. Zarubin,[188] I. Zhizhin,[188] and A. Zhokin[188]

(CMS Collaboration)

[1]*Yerevan Physics Institute, Yerevan, Armenia*
[2]*Institut für Hochenergiephysik, Vienna, Austria*
[3]*Universiteit Antwerpen, Antwerpen, Belgium*
[4]*Vrije Universiteit Brussel, Brussel, Belgium*
[5]*Université Libre de Bruxelles, Bruxelles, Belgium*
[6]*Ghent University, Ghent, Belgium*
[7]*Université Catholique de Louvain, Louvain-la-Neuve, Belgium*
[8]*Centro Brasileiro de Pesquisas Fisicas, Rio de Janeiro, Brazil*
[9]*Universidade do Estado do Rio de Janeiro, Rio de Janeiro, Brazil*
[10]*Universidade Estadual Paulista, Universidade Federal do ABC, São Paulo, Brazil*
[11]*Institute for Nuclear Research and Nuclear Energy, Bulgarian Academy of Sciences, Sofia, Bulgaria*
[12]*University of Sofia, Sofia, Bulgaria*
[13]*Instituto De Alta Investigación, Universidad de Tarapacá, Casilla 7 D, Arica, Chile*
[14]*Beihang University, Beijing, China*
[15]*Department of Physics, Tsinghua University, Beijing, China*
[16]*Institute of High Energy Physics, Beijing, China*
[17]*State Key Laboratory of Nuclear Physics and Technology, Peking University, Beijing, China*
[18]*Sun Yat-Sen University, Guangzhou, China*
[19]*University of Science and Technology of China, Hefei, China*
[20]*Nanjing Normal University, Nanjing, China*
[21]*Institute of Modern Physics and Key Laboratory of Nuclear Physics and Ion-beam Application (MOE)—Fudan University, Shanghai, China*
[22]*Zhejiang University, Hangzhou, Zhejiang, China*
[23]*Universidad de Los Andes, Bogota, Colombia*
[24]*Universidad de Antioquia, Medellin, Colombia*
[25]*University of Split, Faculty of Electrical Engineering, Mechanical Engineering and Naval Architecture, Split, Croatia*
[26]*University of Split, Faculty of Science, Split, Croatia*
[27]*Institute Rudjer Boskovic, Zagreb, Croatia*
[28]*University of Cyprus, Nicosia, Cyprus*
[29]*Charles University, Prague, Czech Republic*
[30]*Escuela Politecnica Nacional, Quito, Ecuador*
[31]*Universidad San Francisco de Quito, Quito, Ecuador*
[32]*Academy of Scientific Research and Technology of the Arab Republic of Egypt, Egyptian Network of High Energy Physics, Cairo, Egypt*
[33]*Center for High Energy Physics (CHEP-FU), Fayoum University, El-Fayoum, Egypt*
[34]*National Institute of Chemical Physics and Biophysics, Tallinn, Estonia*
[35]*Department of Physics, University of Helsinki, Helsinki, Finland*
[36]*Helsinki Institute of Physics, Helsinki, Finland*
[37]*Lappeenranta-Lahti University of Technology, Lappeenranta, Finland*
[38]*IRFU, CEA, Université Paris-Saclay, Gif-sur-Yvette, France*
[39]*Laboratoire Leprince-Ringuet, CNRS/IN2P3, Ecole Polytechnique, Institut Polytechnique de Paris, Palaiseau, France*
[40]*Université de Strasbourg, CNRS, IPHC UMR 7178, Strasbourg, France*
[41]*Institut de Physique des 2 Infinis de Lyon (IP2I), Villeurbanne, France*
[42]*Georgian Technical University, Tbilisi, Georgia*

[43]*RWTH Aachen University, I. Physikalisches Institut, Aachen, Germany*
[44]*RWTH Aachen University, III. Physikalisches Institut A, Aachen, Germany*
[45]*RWTH Aachen University, III. Physikalisches Institut B, Aachen, Germany*
[46]*Deutsches Elektronen-Synchrotron, Hamburg, Germany*
[47]*University of Hamburg, Hamburg, Germany*
[48]*Karlsruher Institut fuer Technologie, Karlsruhe, Germany*
[49]*Institute of Nuclear and Particle Physics (INPP), NCSR Demokritos, Aghia Paraskevi, Greece*
[50]*National and Kapodistrian University of Athens, Athens, Greece*
[51]*National Technical University of Athens, Athens, Greece*
[52]*University of Ioánnina, Ioánnina, Greece*
[53]*HUN-REN Wigner Research Centre for Physics, Budapest, Hungary*
[54]*MTA-ELTE Lendület CMS Particle and Nuclear Physics Group, Eötvös Loránd University, Budapest, Hungary*
[55]*Faculty of Informatics, University of Debrecen, Debrecen, Hungary*
[56]*Institute of Nuclear Research ATOMKI, Debrecen, Hungary*
[57]*Karoly Robert Campus, MATE Institute of Technology, Gyongyos, Hungary*
[58]*Panjab University, Chandigarh, India*
[59]*University of Delhi, Delhi, India*
[60]*Saha Institute of Nuclear Physics, HBNI, Kolkata, India*
[61]*Indian Institute of Technology Madras, Madras, India*
[62]*Tata Institute of Fundamental Research-A, Mumbai, India*
[63]*Tata Institute of Fundamental Research-B, Mumbai, India*
[64]*National Institute of Science Education and Research, An OCC of Homi Bhabha National Institute, Bhubaneswar, Odisha, India*
[65]*Indian Institute of Science Education and Research (IISER), Pune, India*
[66]*Isfahan University of Technology, Isfahan, Iran*
[67]*Institute for Research in Fundamental Sciences (IPM), Tehran, Iran*
[68]*University College Dublin, Dublin, Ireland*
[69a]*INFN Sezione di Bari, Bari, Italy*
[69b]*Università di Bari, Bari, Italy*
[69c]*Politecnico di Bari, Bari, Italy*
[70a]*INFN Sezione di Bologna, Bologna, Italy*
[70b]*Università di Bologna, Bologna, Italy*
[71a]*INFN Sezione di Catania, Catania, Italy*
[71b]*Università di Catania, Catania, Italy*
[72a]*INFN Sezione di Firenze, Firenze, Italy*
[72b]*Università di Firenze, Firenze, Italy*
[73]*INFN Laboratori Nazionali di Frascati, Frascati, Italy*
[74a]*INFN Sezione di Genova, Genova, Italy*
[74b]*Università di Genova, Genova, Italy*
[75a]*INFN Sezione di Milano-Bicocca, Milano, Italy*
[75b]*Università di Milano-Bicocca, Milano, Italy*
[76a]*INFN Sezione di Napoli, Napoli, Italy*
[76b]*Università di Napoli 'Federico II', Napoli, Italy*
[76c]*Università della Basilicata, Potenza, Italy*
[76d]*Scuola Superiore Meridionale (SSM), Napoli, Italy*
[77a]*INFN Sezione di Padova, Padova, Italy*
[77b]*Università di Padova, Padova, Italy*
[77c]*Università di Trento, Trento, Italy*
[78a]*INFN Sezione di Pavia, Pavia, Italy*
[78b]*Università di Pavia, Pavia, Italy*
[79a]*INFN Sezione di Perugia, Perugia, Italy*
[79b]*Università di Perugia, Perugia, Italy*
[80a]*INFN Sezione di Pisa, Pisa, Italy*
[80b]*Università di Pisa, Pisa, Italy*
[80c]*Scuola Normale Superiore di Pisa, Pisa, Italy*
[80d]*Università di Siena, Siena, Italy*
[81a]*INFN Sezione di Roma, Roma, Italy*
[81b]*Sapienza Università di Roma, Roma, Italy*
[82a]*INFN Sezione di Torino, Torino, Italy*

[82b]Università di Torino , Torino, Italy
[82c]Università del Piemonte Orientale , Novara, Italy
[83a]INFN Sezione di Trieste, Trieste, Italy
[83b]Università di Trieste , Trieste, Italy
[84]Kyungpook National University, Daegu, Korea
[85]Department of Mathematics and Physics—GWNU, Gangneung, Korea
[86]Chonnam National University, Institute for Universe and Elementary Particles, Kwangju, Korea
[87]Hanyang University, Seoul, Korea
[88]Korea University, Seoul, Korea
[89]Kyung Hee University, Department of Physics, Seoul, Korea
[90]Sejong University, Seoul, Korea
[91]Seoul National University, Seoul, Korea
[92]University of Seoul, Seoul, Korea
[93]Yonsei University, Department of Physics, Seoul, Korea
[94]Sungkyunkwan University, Suwon, Korea
[95]College of Engineering and Technology, American University of the Middle East (AUM), Dasman, Kuwait
[96]Riga Technical University, Riga, Latvia
[97]University of Latvia (LU), Riga, Latvia
[98]Vilnius University, Vilnius, Lithuania
[99]National Centre for Particle Physics, Universiti Malaya, Kuala Lumpur, Malaysia
[100]Universidad de Sonora (UNISON), Hermosillo, Mexico
[101]Centro de Investigacion y de Estudios Avanzados del IPN, Mexico City, Mexico
[102]Universidad Iberoamericana, Mexico City, Mexico
[103]Benemerita Universidad Autonoma de Puebla, Puebla, Mexico
[104]University of Montenegro, Podgorica, Montenegro
[105]University of Canterbury, Christchurch, New Zealand
[106]National Centre for Physics, Quaid-I-Azam University, Islamabad, Pakistan
[107]AGH University of Krakow, Faculty of Computer Science, Electronics and Telecommunications, Krakow, Poland
[108]National Centre for Nuclear Research, Swierk, Poland
[109]Institute of Experimental Physics, Faculty of Physics, University of Warsaw, Warsaw, Poland
[110]Warsaw University of Technology, Warsaw, Poland
[111]Laboratório de Instrumentação e Física Experimental de Partículas, Lisboa, Portugal
[112]Faculty of Physics, University of Belgrade, Belgrade, Serbia
[113]VINCA Institute of Nuclear Sciences, University of Belgrade, Belgrade, Serbia
[114]Centro de Investigaciones Energéticas Medioambientales y Tecnológicas (CIEMAT), Madrid, Spain
[115]Universidad Autónoma de Madrid, Madrid, Spain
[116]Universidad de Oviedo, Instituto Universitario de Ciencias y Tecnologías Espaciales de Asturias (ICTEA), Oviedo, Spain
[117]Instituto de Física de Cantabria (IFCA), CSIC-Universidad de Cantabria, Santander, Spain
[118]University of Colombo, Colombo, Sri Lanka
[119]University of Ruhuna, Department of Physics, Matara, Sri Lanka
[120]CERN, European Organization for Nuclear Research, Geneva, Switzerland
[121]Paul Scherrer Institut, Villigen, Switzerland
[122]ETH Zurich—Institute for Particle Physics and Astrophysics (IPA), Zurich, Switzerland
[123]Universität Zürich, Zurich, Switzerland
[124]National Central University, Chung-Li, Taiwan
[125]National Taiwan University (NTU), Taipei, Taiwan
[126]High Energy Physics Research Unit, Department of Physics, Faculty of Science, Chulalongkorn University, Bangkok, Thailand
[127]Çukurova University, Physics Department, Science and Art Faculty, Adana, Turkey
[128]Middle East Technical University, Physics Department, Ankara, Turkey
[129]Bogazici University, Istanbul, Turkey
[130]Istanbul Technical University, Istanbul, Turkey
[131]Istanbul University, Istanbul, Turkey
[132]Yildiz Technical University, Istanbul, Turkey
[133]Institute for Scintillation Materials of National Academy of Science of Ukraine, Kharkiv, Ukraine
[134]National Science Centre, Kharkiv Institute of Physics and Technology, Kharkiv, Ukraine
[135]University of Bristol, Bristol, United Kingdom

[136]*Rutherford Appleton Laboratory, Didcot, United Kingdom*
[137]*Imperial College, London, United Kingdom*
[138]*Brunel University, Uxbridge, United Kingdom*
[139]*Baylor University, Waco, Texas, USA*
[140]*Catholic University of America, Washington, DC, USA*
[141]*The University of Alabama, Tuscaloosa, Alabama, USA*
[142]*Boston University, Boston, Massachusetts, USA*
[143]*Brown University, Providence, Rhode Island, USA*
[144]*University of California, Davis, Davis, California, USA*
[145]*University of California, Los Angeles, California, USA*
[146]*University of California, Riverside, Riverside, California, USA*
[147]*University of California, San Diego, La Jolla, California, USA*
[148]*University of California, Santa Barbara—Department of Physics, Santa Barbara, California, USA*
[149]*California Institute of Technology, Pasadena, California, USA*
[150]*Carnegie Mellon University, Pittsburgh, Pennsylvania, USA*
[151]*University of Colorado Boulder, Boulder, Colorado, USA*
[152]*Cornell University, Ithaca, New York, USA*
[153]*Fermi National Accelerator Laboratory, Batavia, Illinois, USA*
[154]*University of Florida, Gainesville, Florida, USA*
[155]*Florida State University, Tallahassee, Florida, USA*
[156]*Florida Institute of Technology, Melbourne, Florida, USA*
[157]*University of Illinois Chicago, Chicago, USA, Chicago, USA*
[158]*The University of Iowa, Iowa City, Iowa, USA*
[159]*Johns Hopkins University, Baltimore, Maryland, USA*
[160]*The University of Kansas, Lawrence, Kansas, USA*
[161]*Kansas State University, Manhattan, Kansas, USA*
[162]*Lawrence Livermore National Laboratory, Livermore, California, USA*
[163]*University of Maryland, College Park, Maryland, USA*
[164]*Massachusetts Institute of Technology, Cambridge, Massachusetts, USA*
[165]*University of Minnesota, Minneapolis, Minnesota, USA*
[166]*University of Mississippi, Oxford, Mississippi, USA*
[167]*University of Nebraska-Lincoln, Lincoln, Nebraska, USA*
[168]*State University of New York at Buffalo, Buffalo, New York, USA*
[169]*Northeastern University, Boston, Massachusetts, USA*
[170]*Northwestern University, Evanston, Illinois, USA*
[171]*University of Notre Dame, Notre Dame, Indiana, USA*
[172]*The Ohio State University, Columbus, Ohio, USA*
[173]*Princeton University, Princeton, New Jersey, USA*
[174]*University of Puerto Rico, Mayaguez, Puerto Rico, USA*
[175]*Purdue University, West Lafayette, Indiana, USA*
[176]*Purdue University Northwest, Hammond, Indiana, USA*
[177]*Rice University, Houston, Texas, USA*
[178]*University of Rochester, Rochester, New York, USA*
[179]*The Rockefeller University, New York, New York, USA*
[180]*Rutgers, The State University of New Jersey, Piscataway, New Jersey, USA*
[181]*University of Tennessee, Knoxville, Tennessee, USA*
[182]*Texas A&M University, College Station, Texas, USA*
[183]*Texas Tech University, Lubbock, Texas, USA*
[184]*Vanderbilt University, Nashville, Tennessee, USA*
[185]*University of Virginia, Charlottesville, Virginia, USA*
[186]*Wayne State University, Detroit, Michigan, USA*
[187]*University of Wisconsin—Madison, Madison, Wisconsin, USA*
[188]*An institute or international laboratory covered by a cooperation agreement with CERN*

[a]Deceased
[b]Also at Yerevan State University, Yerevan, Armenia.
[c]Also at TU Wien, Vienna, Austria.
[d]Also at Institute of Basic and Applied Sciences, Faculty of Engineering, Arab Academy for Science, Technology and Maritime Transport, Alexandria, Egypt.
[e]Also at Ghent University, Ghent, Belgium.

[f]Also at Universidade Estadual de Campinas, Campinas, Brazil.
[g]Also at Federal University of Rio Grande do Sul, Porto Alegre, Brazil.
[h]Also at UFMS, Nova Andradina, Brazil.
[i]Also at Nanjing Normal University, Nanjing, China.
[j]Also at The University of Iowa, Iowa City, Iowa, USA.
[k]Also at University of Chinese Academy of Sciences, Beijing, China.
[l]Also at China Center of Advanced Science and Technology, Beijing, China.
[m]Also at University of Chinese Academy of Sciences, Beijing, China.
[n]Also at China Spallation Neutron Source, Guangdong, China.
[o]Also at Henan Normal University, Xinxiang, China.
[p]Also at Université Libre de Bruxelles, Bruxelles, Belgium.
[q]Also at Another institute or international laboratory covered by a cooperation agreement with CERN.
[r]Also at British University in Egypt, Cairo, Egypt.
[s]Also at Cairo University, Cairo, Egypt.
[t]Also at Purdue University, West Lafayette, Indiana, USA.
[u]Also at Université de Haute Alsace, Mulhouse, France.
[v]Also at Department of Physics, Tsinghua University, Beijing, China.
[w]Also at Tbilisi State University, Tbilisi, Georgia.
[x]Also at The University of the State of Amazonas, Manaus, Brazil.
[y]Also at Erzincan Binali Yildirim University, Erzincan, Turkey.
[z]Also at University of Hamburg, Hamburg, Germany.
[aa]Also at RWTH Aachen University, III. Physikalisches Institut A, Aachen, Germany.
[bb]Also at Isfahan University of Technology, Isfahan, Iran.
[cc]Also at Bergische University Wuppertal (BUW), Wuppertal, Germany.
[dd]Also at Brandenburg University of Technology, Cottbus, Germany.
[ee]Also at Forschungszentrum Jülich, Juelich, Germany.
[ff]Also at CERN, European Organization for Nuclear Research, Geneva, Switzerland.
[gg]Also at Institute of Physics, University of Debrecen, Debrecen, Hungary.
[hh]Also at Institute of Nuclear Research ATOMKI, Debrecen, Hungary.
[ii]Also at Universitatea Babes-Bolyai—Facultatea de Fizica, Cluj-Napoca, Romania.
[jj]Also at MTA-ELTE Lendület CMS Particle and Nuclear Physics Group, Eötvös Loránd University, Budapest, Hungary.
[kk]Also at Physics Department, Faculty of Science, Assiut University, Assiut, Egypt.
[ll]Also at HUN-REN Wigner Research Centre for Physics, Budapest, Hungary.
[mm]Also at Punjab Agricultural University, Ludhiana, India.
[nn]Also at University of Visva-Bharati, Santiniketan, India.
[oo]Also at Indian Institute of Science (IISc), Bangalore, India.
[pp]Also at Birla Institute of Technology, Mesra, Mesra, India.
[qq]Also at IIT Bhubaneswar, Bhubaneswar, India.
[rr]Also at Institute of Physics, Bhubaneswar, India.
[ss]Also at University of Hyderabad, Hyderabad, India.
[tt]Also at Deutsches Elektronen-Synchrotron, Hamburg, Germany.
[uu]Also at Department of Physics, Isfahan University of Technology, Isfahan, Iran.
[vv]Also at Sharif University of Technology, Tehran, Iran.
[ww]Also at Department of Physics, University of Science and Technology of Mazandaran, Behshahr, Iran.
[xx]Also at Helwan University, Cairo, Egypt.
[yy]Also at Italian National Agency for New Technologies, Energy and Sustainable Economic Development, Bologna, Italy.
[zz]Also at Centro Siciliano di Fisica Nucleare e di Struttura Della Materia, Catania, Italy.
[aaa]Also at Università degli Studi Guglielmo Marconi, Roma, Italy.
[bbb]Also at Scuola Superiore Meridionale, Università di Napoli 'Federico II', Napoli, Italy.
[ccc]Also at Fermi National Accelerator Laboratory, Batavia, Illinois, USA.
[ddd]Also at Ain Shams University, Cairo, Egypt.
[eee]Also at Consiglio Nazionale delle Ricerche—Istituto Officina dei Materiali, Perugia, Italy.
[fff]Also at Department of Applied Physics, Faculty of Science and Technology, Universiti Kebangsaan Malaysia, Bangi, Malaysia.
[ggg]Also at Consejo Nacional de Ciencia y Tecnología, Mexico City, Mexico.
[hhh]Also at Trincomalee Campus, Eastern University, Sri Lanka, Nilaveli, Sri Lanka.
[iii]Also at Saegis Campus, Nugegoda, Sri Lanka.
[jjj]Also at National and Kapodistrian University of Athens, Athens, Greece.
[kkk]Also at Ecole Polytechnique Fédérale Lausanne, Lausanne, Switzerland.
[lll]Also at Universität Zürich, Zurich, Switzerland.
[mmm]Also at Stefan Meyer Institute for Subatomic Physics, Vienna, Austria.

[nnn]Also at Laboratoire d'Annecy-le-Vieux de Physique des Particules, IN2P3-CNRS, Annecy-le-Vieux, France.
[ooo]Also at Near East University, Research Center of Experimental Health Science, Mersin, Turkey.
[ppp]Also at Konya Technical University, Konya, Turkey.
[qqq]Also at Izmir Bakircay University, Izmir, Turkey.
[rrr]Also at Adiyaman University, Adiyaman, Turkey.
[sss]Also at Bozok Universitetesi Rektörlügü, Yozgat, Turkey.
[ttt]Also at Marmara University, Istanbul, Turkey.
[uuu]Also at Milli Savunma University, Istanbul, Turkey.
[vvv]Also at Kafkas University, Kars, Turkey.
[www]Also at stanbul Okan University, Istanbul, Turkey.
[xxx]Also at Hacettepe University, Ankara, Turkey.
[yyy]Also at Istanbul University—Cerrahpasa, Faculty of Engineering, Istanbul, Turkey.
[zzz]Also at Yildiz Technical University, Istanbul, Turkey.
[aaaa]Also at Vrije Universiteit Brussel, Brussel, Belgium.
[bbbb]Also at School of Physics and Astronomy, University of Southampton, Southampton, United Kingdom.
[cccc]Also at IPPP Durham University, Durham, United Kingdom.
[dddd]Also at Monash University, Faculty of Science, Clayton, Australia.
[eeee]Also at Università di Torino, Torino, Italy.
[ffff]Also at Bethel University, St. Paul, Minnesota, USA.
[gggg]Also at Karamanoğlu Mehmetbey University, Karaman, Turkey.
[hhhh]Also at California Institute of Technology, Pasadena, California, USA.
[iiii]Also at United States Naval Academy, Annapolis, Maryland, USA.
[jjjj]Also at Bingol University, Bingol, Turkey.
[kkkk]Also at Georgian Technical University, Tbilisi, Georgia.
[llll]Also at Sinop University, Sinop, Turkey.
[mmmm]Also at Erciyes University, Kayseri, Turkey.
[nnnn]Also at Horia Hulubei National Institute of Physics and Nuclear Engineering (IFIN-HH), Bucharest, Romania.
[oooo]Also at Texas A&M University at Qatar, Doha, Qatar.
[pppp]Also at Kyungpook National University, Daegu, Korea.
[qqqq]Also at Universiteit Antwerpen, Antwerpen, Belgium.
[rrrr]Also at Yerevan Physics Institute, Yerevan, Armenia.
[ssss]Also at Northeastern University, Boston, Massachusetts, USA.
[tttt]Also at Imperial College, London, United Kingdom.
[uuuu]Also at Institute of Nuclear Physics of the Uzbekistan Academy of Sciences, Tashkent, Uzbekistan.